## 4.1 Introduction

Docetaxel (as generic or under the trade name Taxotere) is a clinically well-established anti-mitotic chemotherapy medication that works by interfering with cell division.(1–3) Docetaxel is approved by the FDA for treatment of non-small-cell lung cancer, locally advanced or metastatic breast cancer, head and neck cancer, gastric cancer and hormone-refractory prostate cancer. Docetaxel can be used as a single agent or in combination with other chemotherapeutic drugs as indicated depending on specific cancer type and stage. Docetaxel is a member of the taxane drug class, which also includes the chemotherapeutic medication paclitaxel. Although docetaxel remains twice as potent as paclitaxel, the two taxanes have been observed to have comparable efficacy. (4)

Nanoparticles have been extensively studied by researchers in recent years for peroral drug delivery, for systemic effect following uptake from enteron, or to act locally in the gastrointestinal tract. Nanoparticulate delivery systems due to colloidal properties have the potential to improve drug stability, increase the duration of the therapeutic effect, minimise the drug degradation and metabolism as well as cellular efflux.(5–8)

Poly (D,L-lactide-co-glycolide), is a polymer of choice for developing an array of micro and nanoparticulate drug delivery systems as it has excellent biocompatibility and predictable biodegradability(9–11).

PLGA is a copolymer of poly lactic acid (PLA) and poly glycolic acid (PGA). It is the best-defined biomaterial available for drug delivery with respect to design and performance. Poly lactic acid contains an asymmetric α-carbon, which is typically described as the D or L form in classical stereochemical terms and sometimes as R and S form, respectively. The enantiomeric forms of the polymer PLA are poly D-lactic acid (PDLA) and poly L-lactic acid (PLLA). PLGA is generally an acronym for poly D,L-lactic-coglycolic acid where D- and L- lactic acid forms are in equal ratio. The drug delivery specific vehicle, i.e., PLGA, must be able to deliver its payload with appropriate duration, bio-distribution and concentration for the intended therapeutic effect. Therefore, design essentials, including material, geometry and location must incorporate mechanisms of degradation and clearance of the vehicle as well as active pharmaceutical ingredients (API). Bio-distribution and pharmacokinetics of PLGA follows a non-linear and dose-dependent profile. Furthermore, previous studies suggest that both blood

clearance and uptake by the mononuclear phagocyte system (MPS) may depend on dose and composition of PLGA carrier systems. (12–15)

Optimization of pharmaceutical process begins with an objective to find out the and evaluate the independent variables that affect on the formulation response, its determination and to establish their best response values (16–19). However, considering the cost of drugs and polymers, it was desirable to optimize the formulation with minimum batches and maximum desired characteristics. Optimization by changing one variable at a time (OVAT) is a complex method to evaluate the effects of different variables on an experimental outcome. This approach assesses one variable at a time instead of all simultaneously. The method is expensive, time-consuming and often leads to misinterpretation of results when interactions between different components are present. While developing formulations, various formulations as well as process variables related to effectiveness, safety and usefulness should be optimized simultaneously. Quality by design (QBD) is based on the improvement of the quality of formulation at designing level, planned and predefined quality of a formulation (20–23). Studies based on factorial designs allow all the factors to be varied simultaneously, thus enabling evaluation of the effects of each variable at each level and showing interaction among them. It involves stepwise selection of method according to the statistical significance and final model is used to predict relationship between the different variables and their levels. However, such predictions are often limited to low levels, resulting in poor estimation of optimum formulation. Therefore, it is important to understand the complexity of pharmaceutical formulations by using established statistical tools such as multiple regression analysis (MRA), full factorial design etc.(16,17,24,25)

The epidermal growth factor receptor (EGFR) is a member of ErbB family of receptors. It is composed of the extracellular domains, including ligand-binding domain, a tyrosine kinase-containing cytoplasmic region and a hydrophobic transmembrane region (26–29). Stimulation of EGFR by the endogenous ligands, EGF or transforming growth factor-alpha (TGF-alpha), results in to conformational change in receptor, permitting it to enter into the dimers and other oligomers.

Dimerization results in the activation of intracellular tyrosine kinase, protein phosphorylation and stimulation of various cell-signaling pathways that mediate gene transcription and cell cycle progression. The EGFR is expressed on normal human cells but higher levels of expression of the receptor have also been shown to be correlated with malignancy in a variety of cancers. In addition, expression of the EGFR by malignant cells is associated with resistance to therapy and poor prognosis (28,30,31).

Cetuximab is a chimeric human-murine monoclonal antibody that binds competitively and with high affinity to the EGFR (32–34). Binding of the antibody to the EGFR receptor prevents stimulation of the receptor by endogenous ligands and results in inhibition of cell proliferation, enhanced apoptosis, invasiveness, reduced angiogenesis, and metastasis. Binding of cetuximab to the receptor also results in internalization of the antibody-receptor complex, which leads to an overall down regulation of EGFR expression. The EGFR is a prime target for new anticancer therapy, and other agents in development include small molecular tyrosine kinase inhibitors and antisense therapies (26,35,36). In clinical and preclinical studies, cetuximab has been shown to induce response to treatment when used in combination with chemotherapy in patients previously refractory to chemotherapy. Based on these studies, cetuximab can be added to regimens using docetaxel, cisplatin, carboplatin, irinotecan, paclitaxel and fluorouracil and may add to treatment efficacy (37). Phase I range finding studies showed that saturation of cetuximab clearance occurred after administration of 400 $mg/m^2$ as a loading dose followed by weekly infusions of 250 $mg/m^2$. The most commonly reported adverse event associated with cetuximab treatment is an acneiform rash that occurs in 70-80% of patients treated with cetuximab (32,33,38). The rash is rarely dose or treatment limiting, and may diminish in intensity with continued exposure to cetuximab. Improvement may be seen after treatment with topical steroids or topical retinoid and topical antibiotic preparations

## 4.2 Preparation of Docetaxel-Loaded Nanoparticles by Emulsification Solvent Evaporation Method

### 4.2.1 Method:

The Emulsification Solvent Evaporation method was employed for preparation of PLGA NPs containing docetaxel. Briefly, docetaxel and PLGA were dissolved in acetone as an organic solvent that is miscible with water. The drug-polymer solution was then added to an aqueous phase containing 0.5% PVA (W/V). The mixture was probe sonicated (Cole-Parmer 750-Watt Ultrasonic Homogenizer with Temp Controller) at 5 amplitudes for 60 seconds to produce an O/W emulsion. The O/W emulsion was stirred using a magnetic stirrer for 4 hours at room temperature until the evaporation of the organic phase was completed to generate NPs. The NPs were then collected by ultracentrifugation for 15 min at 50,000 g. The PLGA NPs were re-suspended, washed with water, and collected similarly.(39–41) A stepwise process is given in Figure 4.1 as a process flow chart.

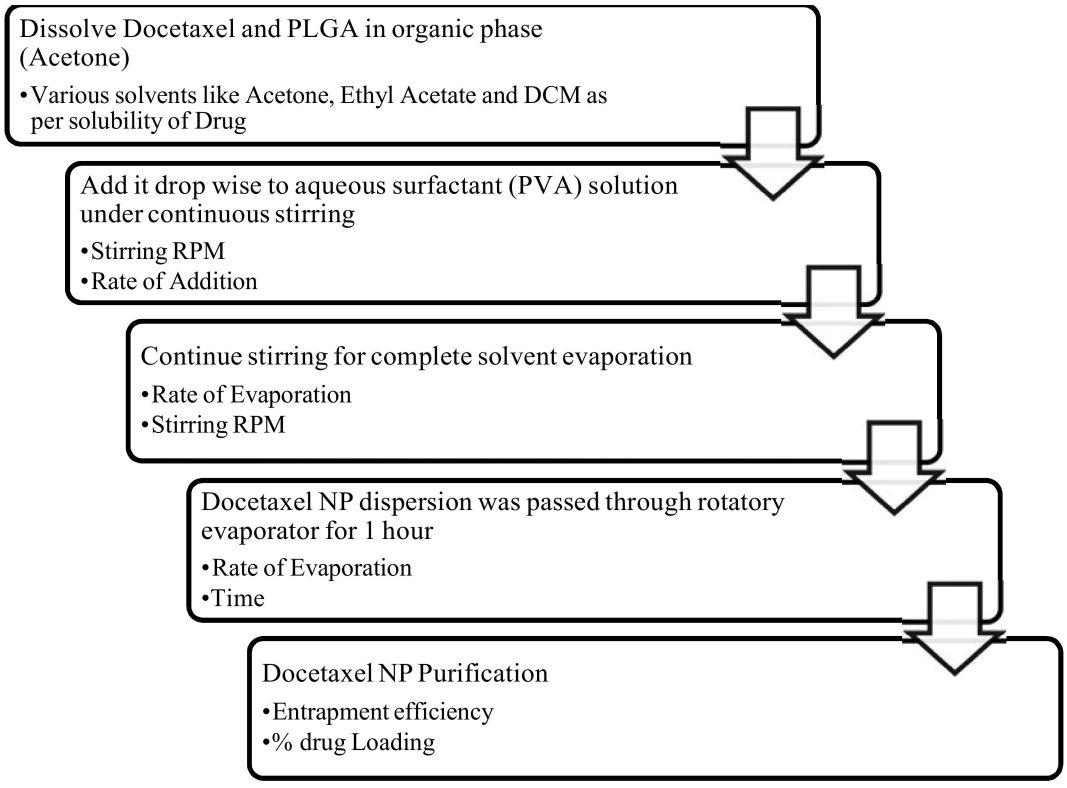


**Figure 4.1 Process Flowchart**

**4.3 Preliminary Optimization of Parameters:**

In preliminary optimization, the possible parameters influencing the formation of nanoparticles, size of nanoparticles and entrapment efficiency were identified and optimized. The aim of this work is to optimize and characterize the formulation prepared by emulsification solvent evaporation method for the preparation of nanoparticles in order to identify formulation and process parameters.(16,17,19,23)

Preliminary experiments and research studies have indicated that the variables mostly affecting the preparation of PLGA NPs by nanoprecipitation technique were the amounts of polymer, concentration of the drug, the ratio of organic to aqueous phase. Box-Behnken design was particularly used to statistically optimize the formulation parameters and evaluate the main interaction effects since it requires a small number of runs in case of three or four variables. A 3-factor, 3-level Box-Behnken design was used to optimize NP formulation with polymer concentration (X1), drug concentration (X2) and the ratio of organic to aqueous solvent (X3) as the independent variables with low, medium and high concentration values presented in Table 4.1.

The Box-Behnken designs 17 experiments, including 12 factorial points, with 5 replicates at the center point for estimation of pure error sum of squares, were employed.(19,22,42,43)

**4.4 Optimization by Factorial Design**(16,17,43)

Based on the preliminary experiments, the polymer concentration (X1), Drug Concentration (X2) and Ratio of Solvent to Water (X3) were selected as independent variables and particle size (PS), PDI and % Drug Loading were selected as dependent variables. A 33 randomized full factorial design was used. In this design, three factors were evaluated, each at 3 levels, and experimental trials were performed at all 27 possible combinations with two replicates. Replicate experimental runs were carried out in a complete randomized manner.

**Table 4.1 Variables in Box–Behnken design**

| Factor | Levels used | | |
|---|---|---|---|
| ***Independent variables*** | *-1* | *0* | *+1* |
| X1:Polymer Concentration (mg/ml) | 5 | 10 | 15 |
| X2:Drug Concentration (mg/ml) | 0.5 | 1.0 | 2 |
| X3:Ratio of Solvent to Water | 0.1 | 0.3 | 0.5 |

| **Dependent variables** | **Contriants** |
|---|---|
| Particle Size (nm) | Minimize |
| PDI | Minimize |
| % Drug Loading | Maximize |

**Table 4.2 Formulation of Docetaxel loaded nanoparticles with coded values**

| Batch Code | X1 | X2 | X3 |
|---|---|---|---|
| F1 | -1.000 | 0.000 | 1.000 |
| F2 | 0.000 | 0.000 | 0.000 |
| F3 | -1.000 | -1.000 | 0.000 |
| F4 | 1.000 | 1.000 | 0.000 |
| F5 | 0.000 | 0.000 | 0.000 |
| F6 | 1.000 | 0.000 | 1.000 |
| F7 | -1.000 | 0.000 | -1.000 |
| F8 | 1.000 | 0.000 | -1.000 |
| F9 | 0.000 | -1.000 | 1.000 |
| F10 | 0.000 | 1.000 | 1.000 |

| | | | |
|---|---|---|---|
| F11 | 0.000 | 0.000 | 0.000 |
| F12 | 0.000 | 1.000 | -1.000 |
| F13 | 0.000 | 0.000 | 0.000 |
| F14 | 1.000 | -1.000 | 0.000 |
| F15 | 0.000 | -1.000 | -1.000 |
| F16 | -1.000 | 1.000 | 0.000 |
| F17 | 0.000 | 0.000 | 0.000 |

A multilinear stepwise regression analysis was performed using Microsoft Excel software. All the statistical operations were carried out by design expert (8.0.7.1, Stat-Ease, Inc.. Minneapolis, USA). Table 4.1 and Table 4.2 summarize experimental runs studied, their factor combinations, and the translation of the coded levels to the experimental units employed during the study.

Various RSM (Response Surface Methodology) computations for optimization study were performed employing Design Expert® software (version 8.0.7.1, Stat-Ease Inc, Minneapolis, USA). Polynomial models including interaction and quadratic terms were generated for the response variable using multiple regression analysis (MLRA) approach. The general form of MLRA model is represented as equation 4.1.

$$Y = b_0 + b_1X_1 + b_2X_2 + b_3X_3 + b_{12}X_1X_2 + b_{13}X_1X_3 + b_{23}X_2X_3 + b_{12}X_{11} + b_{22}X_{22} + b_{32}X_{33} + b_{123}X_1X_2X_3 \quad (4.1)$$

Where $b_0$ is the intercept representing the arithmetic average of all quantitative outcomes of 27 runs; bij are the coefficients computed from the observed experimental values of Y; and $X_1$, $X_2$ and $X_3$ are the coded levels of the independent variable(s). The terms $X_1X_2$ and $Xi_2$ (i =1to3) represents the interaction and quadratic terms, respectively. The main effects ($X_1$, $X_2$ and $X_3$) represent the average result of changing one factor at a time from its low to high value. The interaction terms ($X_1X_2X_3$) show how the response changes when three factors are simultaneously changed. The polynomial terms ($X_{12}$, $X_{22}$ and $X_{32}$) are included to investigate nonlinearity. The polynomial equation was used to draw conclusions after considering the magnitude of the coefficients and the mathematical sign it carries, i.e., positive or negative. A positive sign signifies a positive interaction, whereas a negative sign stands for negative interaction. The effects of different levels of independent variables on the response parameters were predicted from the respective response surface plots.

The predicted values were calculated by using the mathematical model based on the coefficients of the model and the predicted values along with their observed values were recorded along with percentage of error obtained when predicted value and observed values were compared. The statistical validity of the polynomials was established on the basis of ANOVA provision in the Design Expert ®software.(21) Level of significance was considered at $P<0.05$. F-Statistic was applied on the results of analysis of variance (ANOVA) of full model and reduced model to check whether the non-significant terms can be omitted or not from the FM. The best fitting mathematical model was selected based on the comparisons of several statistical parameters including the coefficient of variation (CV), the multiple correlation coefficient (R2), adjusted multiple correlation coefficient (adjusted R2). For simultaneous optimization of PS and % Drug Loading, desirability function (multi-response optimization technique) was applied and total desirability was calculated. A check point analysis was performed to confirm the utility of the multiple regression analysis and established contour plots in the preparation of Docetaxel loaded PLGA NPs. Results of desirability criteria, check point analysis and normalized error were considered to select the formulation with lowest PS and highest % Drug Loading.

**4.5 Lyophilization of Docetaxel Loaded Nanoparticles and Optimization of Cryoprotectant**

The optimized nanoparticle formulation was lyophilized using freeze dryer. Different cryoprotectants (Trehalose, Mannitol and Sucrose) at different ratio of Docetaxel Loaded Nanoparticles to Cryoprotectant (1:1 w/w, 1:2 w/w, 1:3 w/w) were tried to select the cryoprotectant which showed a minimum increment in particle size. Nanoparticulate suspension (2 ml) was dispensed in 10 ml semi-stoppered vials with rubber closures and frozen for 24 hours at -80°C. Thereafter, the vials are lyophilized using trehalose, sucrose and mannitol in different concentrations. Finally, glass vials were sealed under anhydrous conditions and stored until being re-hydrated. Lyophilized NPs were re-suspended in exactly the same volume of distilled water as before lyophilization. NP suspension was subjected to particle size measurement as described earlier. Ratio of the final particle size and initial particle size (Si) was calculated to finalize the suitable cryoprotectant based upon lowest Sf/Si ratio.

### 4.6 Characterization of Optimized Docetaxel Loaded Nanoparticles

#### 4.6.1 Particle Size

The size analysis and polydispersity index of the Nanoparticles were determined using a Malvern Zetasizer Nano ZS (Malvern Instrument, UK). Each sample was diluted ten times with distilled water to avoid multi-scattering phenomena and placed in the cuvette. Polydispersity index was noted to determine the narrow particle size distribution. Analysis was performed in triplicate and the results were expressed as mean size ± SD.(8)

#### 4.6.2 Entrapment Efficiency and Drug Loading

Drug loading in the Nanoparticles was determined after separating the Nanoparticles present in the aqueous supernatant (containing entrapped Docetaxel) by centrifugation at 5000 rpm for 10 min. Acetonitrile was added to the Nanoparticles to dissolve the polymer and centrifuged. The supernatant was diluted with the appropriate amount of purified water and analyzed for entrapped drug by spectrophotometer after filtration through 0.22 µ and appropriate dilution. The precipitated drug was settled down at centrifuge tube was removed and dissolved in acetonitrile and the drug was analyzed for the free drug content. Drug loading was estimated by calculating amount of drug entrapped in NPs with respect to total drug added during preparation of formulation.

The Entrapment was calculated according to following formula:

$$\text{Entrapment}(\%) = \frac{\text{Total amount of drug added} - \text{amount of entrapped drug}}{\text{amount of entrapped drug}} X100$$

Drug loading was calculated as follows,

$$\text{Drug loading}(\%) = \frac{\text{Drug content in the Nanoparticles}}{\text{Weight of Nanoparticles}} X100$$

#### 4.6.3 Zeta Potential

Zeta potential distribution was also measured using a Zetasizer (Nano ZS, Malvern instrument, Worcestershire, UK). Each sample was suitably diluted 10 times with distilled water and placed in a disposable cell. The electrophoretic mobility (µm/sec) was converted to zeta potential by using Helmholtz-Smoluchowski equation. An average of 3 measurements of each sample was used to derive average zeta potential.(44,45)

## 4.7 Results and Discussion

### 4.7.1 Optimization by Factorial Design

For the purpose of nanoparticle formulation optimization, three-dimensional response surface plots from the experimental data were drawn. All responses observed were fitted to linear, second order and quadratic models, and were evaluated in expressions of statistically significant coefficients p-values and R2 values. Polynomial equations relating the major effect and interface factors were determined based on evaluation of statistical parameters such as multiple correlation coefficient, adjusted multiple correlation coefficient and the predicted residual sum of squares generated by Design-Expert software. The statistical corroboration of the polynomial equations was established by ANOVA through Fisher's test and shown by a p value below 0.05, which is provision available in the software. Therefore, the optimum values of the variables were obtained by graphical and numerical analyses using the Design-Expert software and based on the criterion of desirability. In order to graphically show the relationship and interactions between the coded variables and the response, contour plots and three-dimensional surface plots were used in this study. The optimal points were determined by solving the equation derived from the final quadratic model and grid search of RSM plot. NPs were organized using the optimal formulation, and resultant experimental values of the responses were quantitatively compared with the predicted values for calculating the percentage of the predicted error. Predicted error is the variation between the experimental value and the predicted value per predicted value. Validation of the optimization procedure was demonstrated for predicted errors lower than 5%. Formulation Composition and observed responses during experimnetation are provided in Table 4.3.

**Table 4.3 Composition and observed responses in Box–Behnken design**

| | Factor 1 | Factor 2 | Factor 3 | Response 1 | Response 2 | Response 3 |
|---|---|---|---|---|---|---|
| Run | A:Polymer Concentration (mg/mL) | B:Drug Concentration (mg/mL) | C:Ratio of Solvent to Water | Particle Size (nm) | PDI | % Drug Loading |
| 1 | 5.00 | 1.00 | 0.50 | 178 | 0.3 | 5.39 |
| 2 | 10.00 | 1.00 | 0.30 | 184 | 0.3 | 7.22 |
| 3 | 5.00 | 0.50 | 0.30 | 158 | 0.1 | 0.17 |

| | | | | | | |
|---|---|---|---|---|---|---|
| 4 | 15.00 | 2.00 | 0.30 | 203 | 0.2 | 3.7 |
| 5 | 10.00 | 1.00 | 0.30 | 185 | 0.2 | 8.56 |
| 6 | 15.00 | 1.00 | 0.50 | 241 | 0.4 | 1.15 |
| 7 | 5.00 | 1.00 | 0.10 | 185 | 0.1 | 2 |
| 8 | 15.00 | 1.00 | 0.10 | 214 | 0.2 | 1.46 |
| 9 | 10.00 | 0.50 | 0.50 | 186 | 0.2 | 0.4 |
| 10 | 10.00 | 2.00 | 0.50 | 207 | 0.25 | 5.04 |
| 11 | 10.00 | 1.00 | 0.30 | 218 | 0.15 | 9.03 |
| 12 | 10.00 | 2.00 | 0.10 | 206 | 0.12 | 5.23 |
| 13 | 10.00 | 1.00 | 0.30 | 243 | 0.16 | 7.71 |
| 14 | 15.00 | 0.50 | 0.30 | 224 | 0.2 | 0.15 |
| 15 | 10.00 | 0.50 | 0.10 | 180 | 0.12 | 0.14 |
| 16 | 5.00 | 2.00 | 0.30 | 180 | 0.12 | 11.54 |
| 17 | 10.00 | 1.00 | 0.30 | 210 | 0.2 | 8.2 |

***i. Statistical Analysis of Response Particle Size***

p-value of the different models, p-value for lack of fit in the model, Adjusted R2 value and Predicted R2 values are shown in the following **Table 4.4**.

**Table 4.4 Summary of ANOVA results for Different Models**

| | Sequential | Lack of Fit | Adjusted | Predicted | |
|---|---|---|---|---|---|
| Source | p-value | p-value | R-Squared | R-Squared | |
| Linear | 0.0013 | 0.7222 | 0.6167 | 0.4781 | Suggested |
| 2FI | 0.3792 | 0.7444 | 0.6288 | 0.3483 | |
| Quadratic | 0.4824 | 0.7351 | 0.6188 | 0.1387 | |
| Cubic | 0.7351 | | 0.4993 | | Aliased |

As it can be seen from the **Table 4.4**, the best model to fit the experimental results of Particle Size in nanoparticles is linear model. The higher model (cubic model) is significant ($p<0.05$) but the non-agreement between the adjusted R2 value and predicted

R2 value and aliased structure of response prediction rules out the cubic model. **Table 4.5** below shows the ANOVA analysis of the suggested linear model.

**Table 4.5 ANOVA Table for Response Surface linear Model**

| Source | Sum of Squares | df | Mean Square | F Value | p-value Prob > F | |
|---|---|---|---|---|---|---|
| Model | 5712.75 | 6 | 952.13 | 5.52 | 0.0092 | significant |
| *A-Polymer Concentration* | *4802.00* | *1* | *4802.00* | *27.83* | *0.0004* | |
| *B-Drug Concentration* | *288.00* | *1* | *288.00* | *1.67* | *0.2255* | |
| *C-Ratio of Solvent to Water* | *32.00* | *1* | *32.00* | *0.19* | *0.6759* | |
| *AB* | *306.25* | *1* | *306.25* | *1.77* | *0.2124* | |
| *AC* | *272.25* | *1* | *272.25* | *1.58* | *0.2377* | |
| *BC* | *12.25* | *1* | *12.25* | *0.071* | *0.7953* | |
| Residual | 1725.72 | 10 | 172.57 | | | |
| *Lack of Fit* | *794.52* | *6* | *132.42* | *0.57* | *0.7444* | *not significant* |
| *Pure Error* | *931.20* | *4* | *232.80* | | | |
| Cor Total | 7438.47 | 16 | | | | |

The Model F-value of 5.52 implies the model is significant. There is only a 0.01 % chance that a "Model F-Value" this large could occur due to noise. Values of "Prob > F" less than 0.0500 indicate model terms are significant. In this case A is significant model term. This signifies that Polymer Concentration have significant effect on Particle Size. Polymer Concentration shows linear effect in the response. Values greater than 0.1000 indicate the model terms are not significant. The "Lack of Fit F-value" of 0.57 implies the Lack of Fit is not significant relative to the pure error. There is a 74.44 % chance that a "Lack of Fit F-value" this large could occur due to noise. Non-significant lack of fit implies that selected linear model fits the responses.

**Table 4.6 Summary of ANOVA results for Quadratic Model**

| | | | |
|---|---|---|---|
| Std. Dev. | 13.14 | R-Squared | 0.7680 |
| Mean | 197.82 | Adj R-Squared | 0.6288 |
| C.V. % | 6.64 | Pred R-Squared | 0.3483 |
| PRESS | 4847.44 | Adeq Precision | 8.779 |

Effect of polymer concentration, drug concentration and ratio of solvent to water on Particle size are presented in Figure 4.2, Figure 4.3 and Figure 4.4 respectively.

Summary of ANOVA results for selected linear model is shown in **Table 4.6**. The "Pred RSquared" of 0.3483 is in reasonable agreement with the "Adj R-Squared" of 0.6288. "Adeq Precision" measures the signal to noise ratio. A ratio greater than 4 is desirable. Here ratio of 8.779 indicates an adequate signal. This model can be used to navigate the design space.

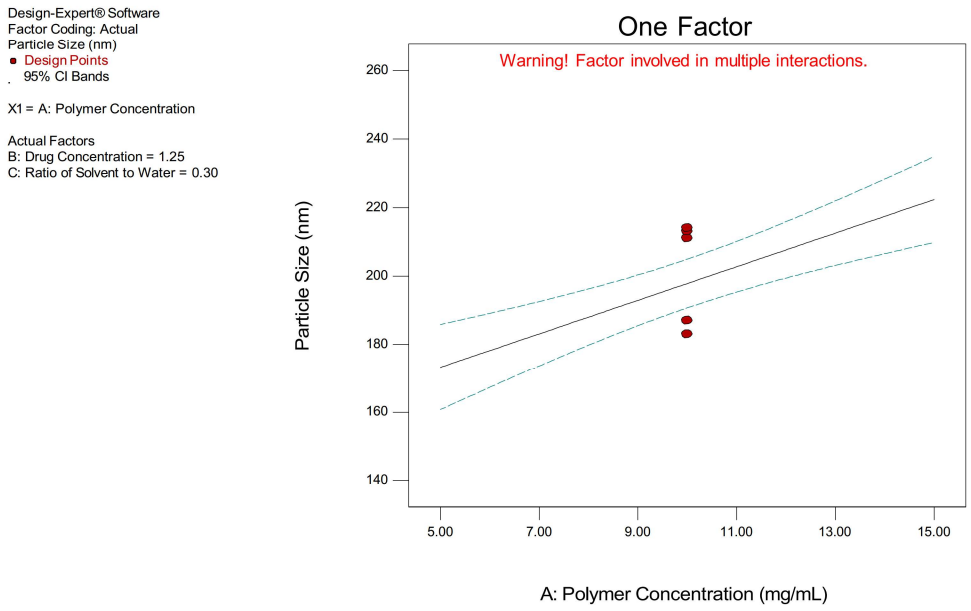


**Figure 4.2 Effect of polymer concentration on Particle size**

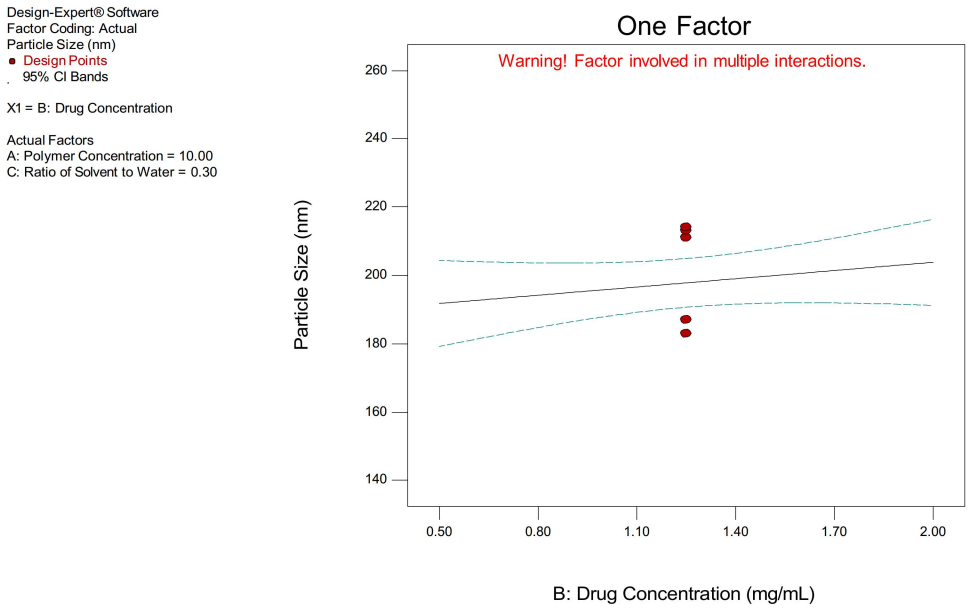


**Figure 4.3 Effect of drug concentration on Particle size**

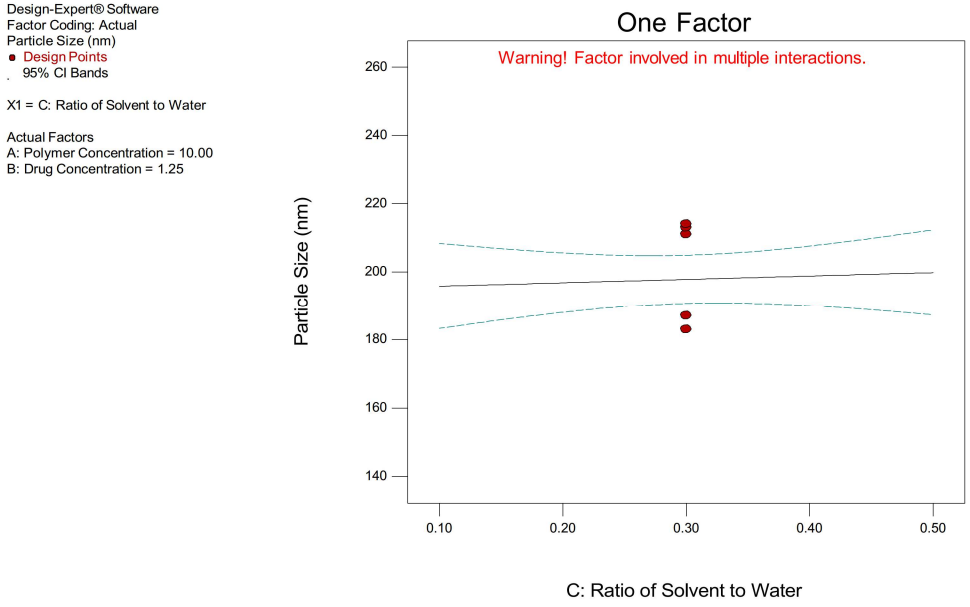


**Figure 4.4 Effect of ratio of solvent to water on Particle size**

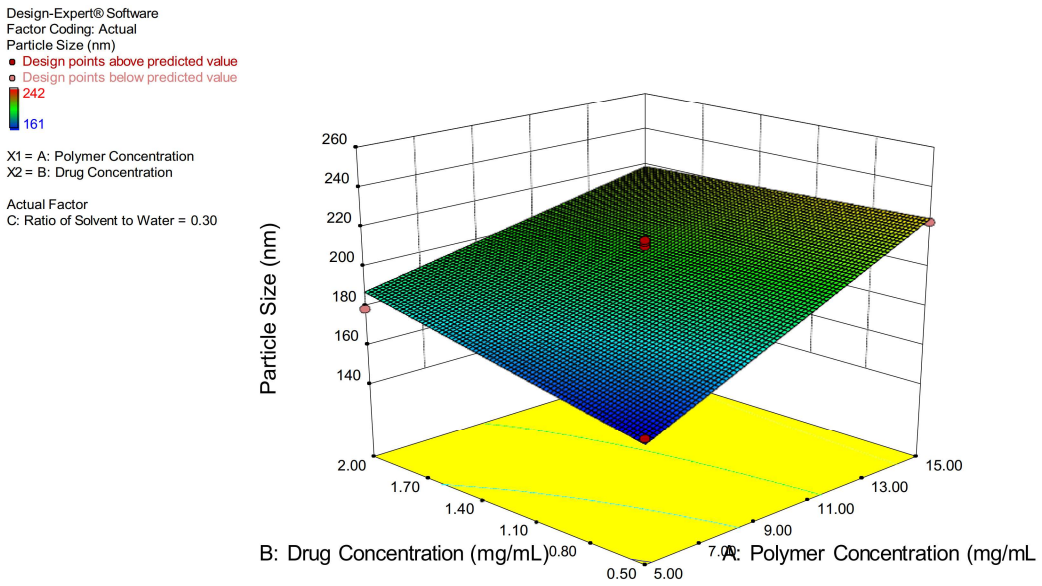


**Figure 4.5 Response surface showing combined effect of drug concentration and polymer concentration on Particle size**

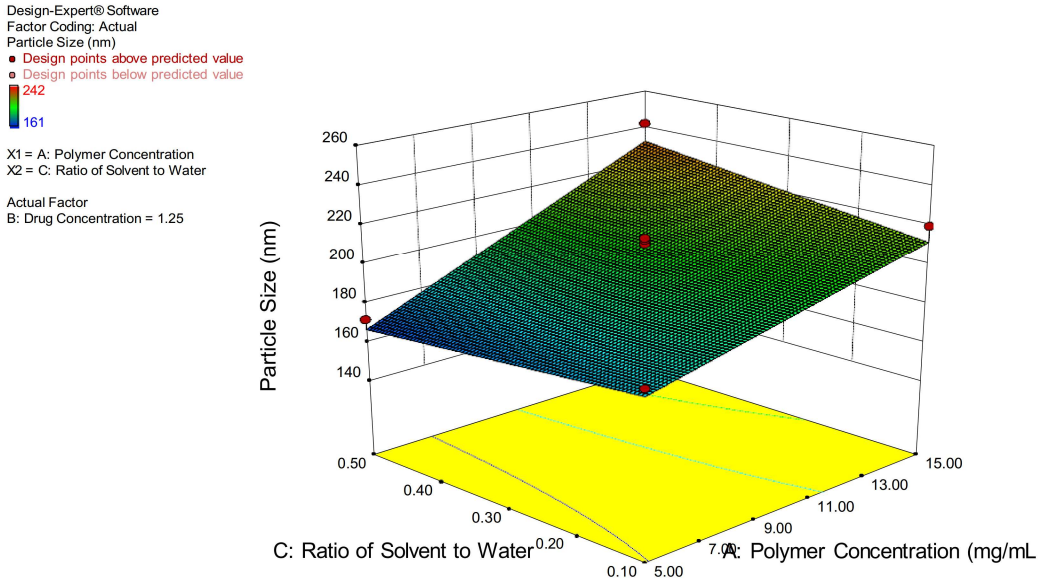


**Figure 4.6 Response surface showing combined effect of Ratio of Solvent to Water and polymer concentration on Particle size**

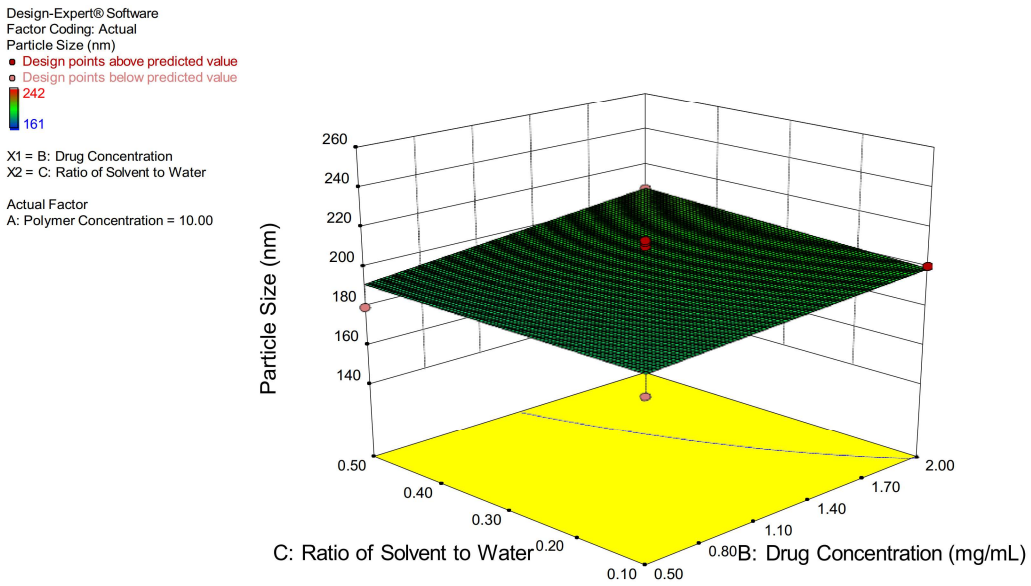


**Figure 4.7 Response surface showing combined effect of Ratio of Solvent to Water and drug concentration on Particle size**

**Predicted response at any point of the plot can be represented by the following equation:**

Particle Size =

+135.78186

+5.34167 * Polymer Concentration

+27.83333 * Drug Concentration

-87.08333 * Ratio of Solvent to Water

-2.33333 * Polymer Concentration * Drug Concentration

+8.25000 * Polymer Concentration * Ratio of Solvent to Water

+11.66667 * Drug Concentration * Ratio of Solvent to Water

***ii. Statistical Analysis of PDI***

p-value of the different models, p-value for lack of fit in the model, Adjusted R2 value and Predicted R2 values are shown in the following Table 4.8.

**Table 4.7 Summary of ANOVA results for Different Models**

| | Sequential | Lack of Fit | Adjusted | Predicted | |
|---|---|---|---|---|---|
| Source | p-value | p-value | R-Squared | R-Squared | |
| Linear | 0.0068 | 0.4832 | 0.5028 | 0.2668 | Suggested |
| 2FI | 0.8937 | 0.3415 | 0.3903 | -0.4907 | |
| Quadratic | 0.0636 | 0.7875 | 0.6728 | 0.3389 | Suggested |
| Cubic | 0.7875 | | 0.5486 | | Aliased |

As it can be seen from the **Table 4.7**, the best model to fit the experimental results of PDI in nanoparticles is linear model. The higher model (Quadratic model) is significant ($p<0.05$) but the non-agreement between the adjusted R2 value and predicted R2 value and and aliased structure of response prediction rules out the Quadratic model. **Table 4.8** below shows the ANOVA analysis of the suggested linear model.

**Table 4.8 ANOVA Table for Response Surface linear Model**

| | Sum of | | Mean | F | p-value | |
|---|---|---|---|---|---|---|
| Source | Squares | df | Square | Value | Prob > F | |
| Model | 0.084 | 9 | 9.348E-003 | 4.66 | 0.0274 | significant |
| *A-Polymer Concentration* | *0.017* | *1* | *0.017* | *8.52* | *0.0224* | |
| *B-Drug Concentration* | *8.000E-004* | *1* | *8.000E-004* | *0.40* | *0.5479* | |
| *C-Ratio of Solvent to Water* | *0.041* | *1* | *0.041* | *20.23* | *0.0028* | |
| *AB* | *2.250E-004* | *1* | *2.250E-004* | *0.11* | *0.7476* | |
| *AC* | *1.388E-017* | *1* | *1.388E-017* | *6.912E-015* | *1.0000* | |
| *BC* | *2.025E-003* | *1* | *2.025E-003* | *1.01* | *0.3487* | |
| *A^2* | *5.568E-004* | *1* | *5.568E-004* | *0.28* | *0.6147* | |
| *B^2* | *0.018* | *1* | *0.018* | *9.13* | *0.0193* | |
| *C^2* | *5.609E-003* | *1* | *5.609E-003* | *2.79* | *0.1386* | |
| Residual | 0.014 | 7 | 2.008E-003 | | | |

| | | | | | | |
|---|---|---|---|---|---|---|
| *Lack of Fit* | *2.975E-003* | *3* | *9.917E-004* | *0.36* | *0.7875* | *not significant* |
| *Pure Error* | *0.011* | *4* | *2.770E-003* | | | |
| Cor Total | 0.098 | 16 | | | | |

The Model F-value of 4.66 implies the model is significant. There is only a 2.74% chance that an F-value this large could occur due to noise. Values of "Prob > F" less than 0.0500 indicate model terms are significant.

In this case A, C, B^2 are significant model terms. Values greater than 0.1000 indicate the model terms are not significant. If there are many insignificant model terms (not counting those required to support hierarchy), model reduction may improve your model. The "Lack of Fit F-value" of 0.36 implies the Lack of Fit is not significant relative to the pure error. There is a 78.75% chance that a "Lack of Fit F-value" this large could occur due to noise. Non-significant lack of fit is good -- we want the model to fit.

**Table 4.9 Summary of ANOVA results for Quadratic Model**

| | | | |
|---|---|---|---|
| Std. Dev. | 0.045 | R-Squared | 0.8569 |
| Mean | 0.19 | Adj R-Squared | 0.6728 |
| C.V. % | 23.15 | Pred R-Squared | 0.3389 |
| PRESS | 0.065 | Adeq Precision | 8.256 |

The "Pred R-Squared" of 0.3389 is not as close to the "Adj R-Squared" of 0.6728 as one might normally expect; i.e. the difference is more than 0.2. This may indicate a large block effect or a possible problem with your model and/or data. Things to consider are model reduction, response transformation, outliers, etc. All empirical models should be tested by doing confirmation runs. "Adeq Precision" measures the signal to noise ratio. A ratio greater than 4 is desirable. Your ratio of 8.256 indicates an adequate signal. This model can be used to navigate the design space.

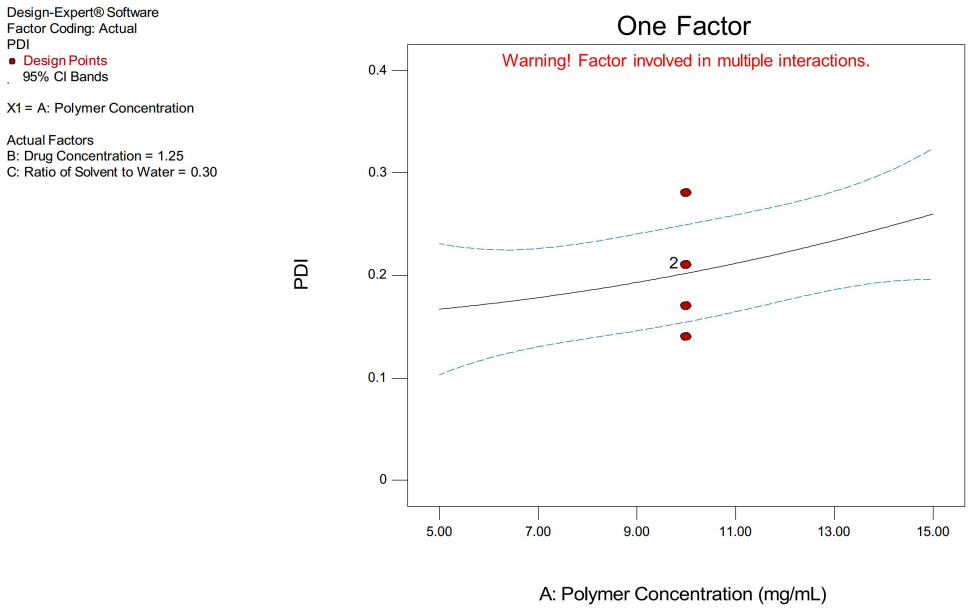


**Figure 4.8 Effect of polymer concentration on PDI**

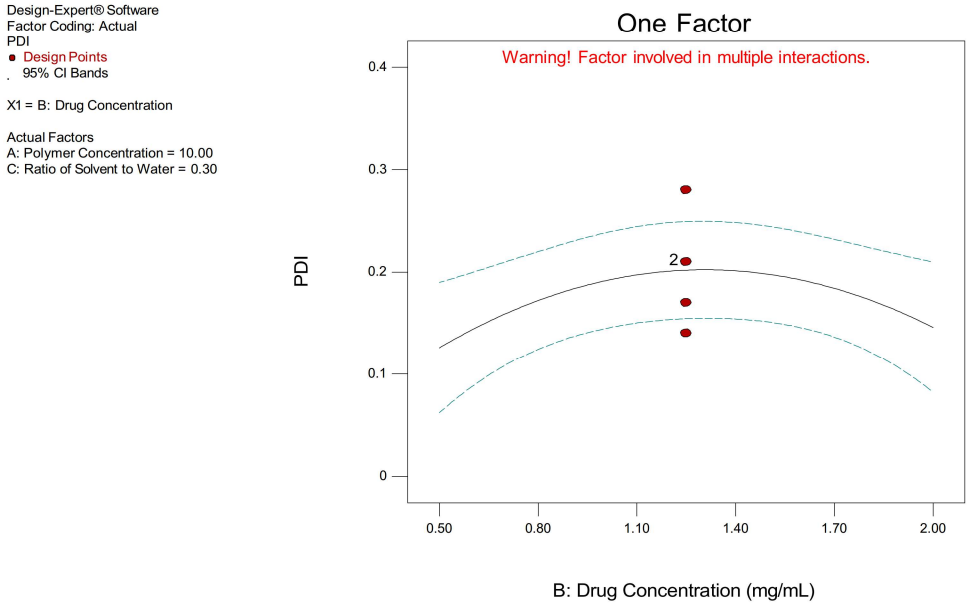


**Figure 4.9 Effect of drug concentration on PDI**

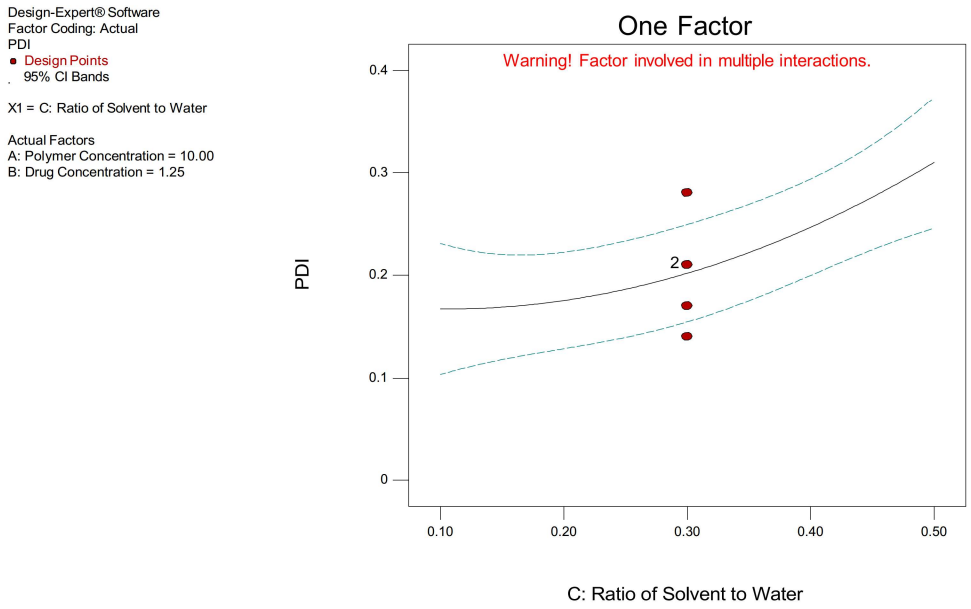


**Figure 4.10 Effect of ratio of solvent to water on PDI**

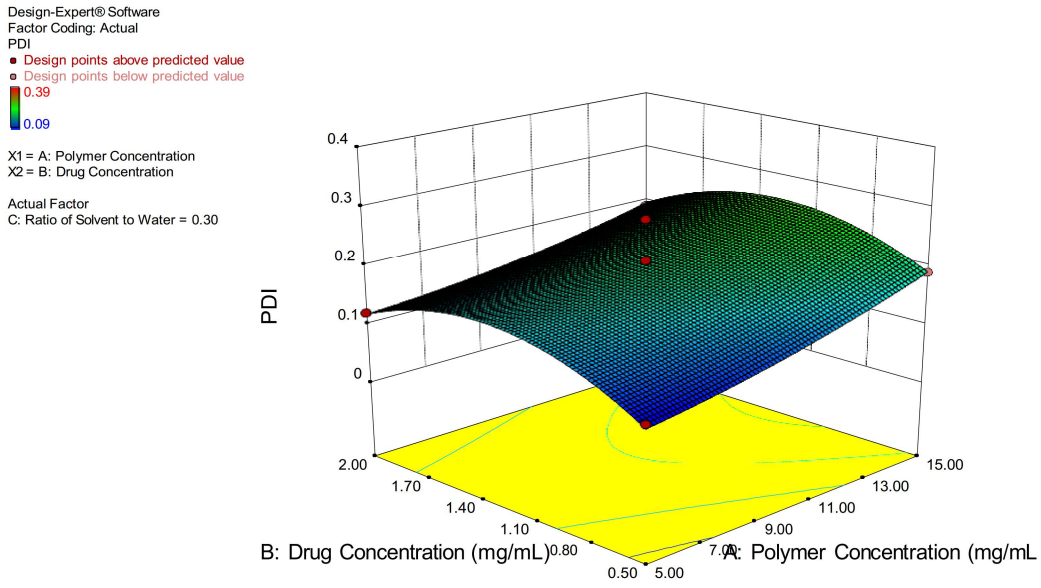


**Figure 4.11 Response surface showing combined effect of drug concentration and polymer concentration on PDI**

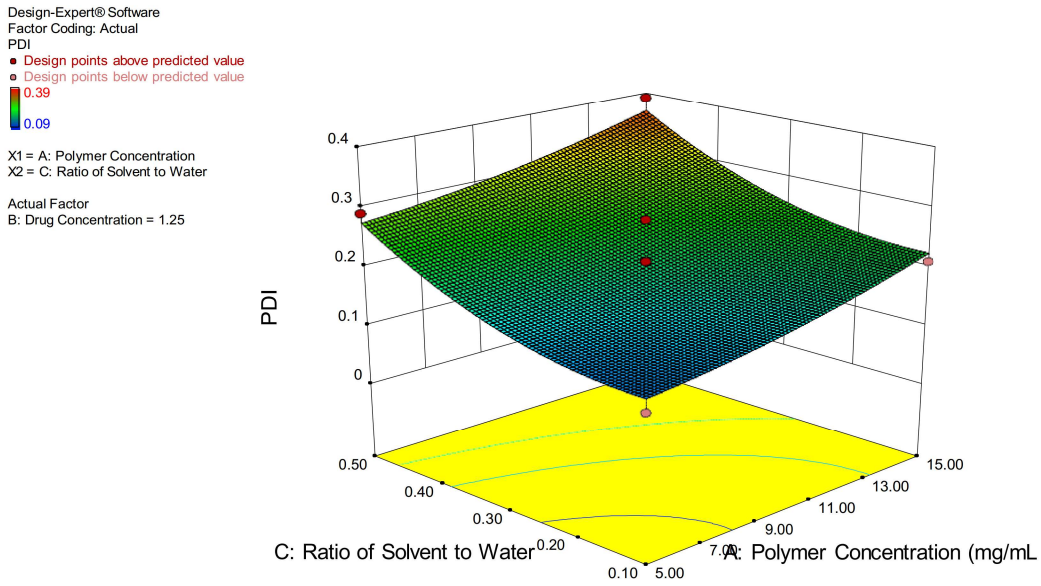


**Figure 4.12 Response surface showing combined effect of Ratio of Solvent to Water and polymer concentration on PDI**

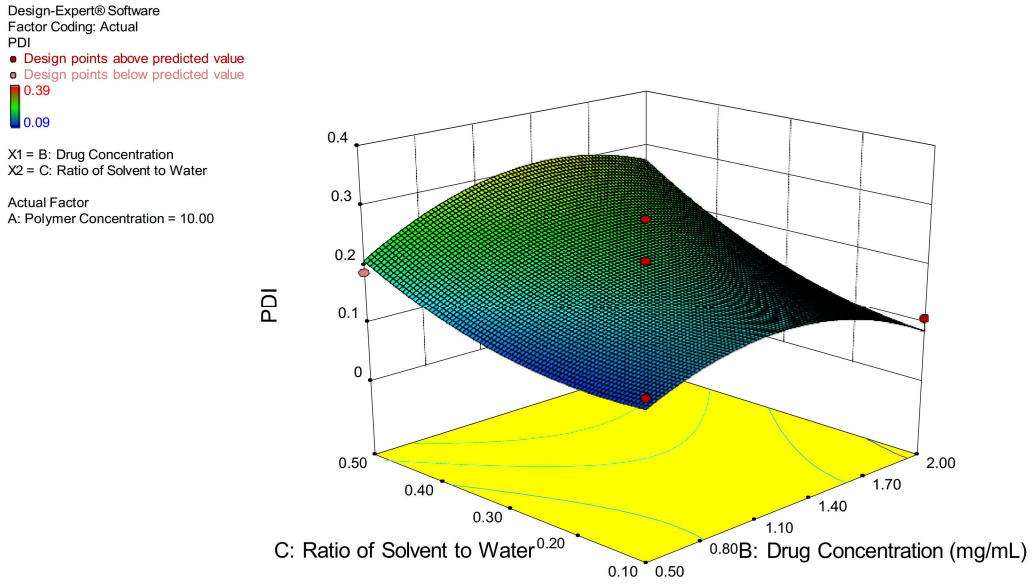


**Figure 4.13 Response surface showing combined effect of Ratio of Solvent to Water and drug concentration on PDI**

**Predicted response at any point of the plot can be represented by the following equation:**

PDI =

-0.038000

+2.55000E-003 * Polymer Concentration

+0.28167 * Drug Concentration

-0.37875 * Ratio of Solvent to Water

-2.00000E-003 * Polymer Concentration * Drug Concentration

+5.99822E-018 * Polymer Concentration * Ratio of Solvent to Water

+0.15000 * Drug Concentration * Ratio of Solvent to Water

+4.60000E-004 * Polymer Concentration^2

-0.11733 * Drug Concentration^2

+0.91250 * Ratio of Solvent to Water^2

***iii. Statistical Analysis of % drug loading***

p-value of the different models, p-value for lack of fit in the model, Adjusted R2 value and Predicted R2 values are shown in the following Table 4.10.

**Table 4.10 Summary of ANOVA results for Different Models**

| | **Sequential** | **Lack of Fit** | **Adjusted** | **Predicted** | |
|---|---|---|---|---|---|
| **Source** | **p-value** | **p-value** | **R-Squared** | **R-Squared** | |
| Linear | 0.0145 | 0.0799 | 0.4374 | 0.2922 | |
| 2FI | 0.6013 | 0.0590 | 0.3878 | 0.0693 | |
| Quadratic | 0.0033 | 0.6404 | 0.8636 | 0.6346 | Suggested |
| Cubic | 0.6404 | | 0.8366 | | Aliased |

As it can be seen from the **Table 4.10**, the best model to fit the experimental results of % drug loading in nanoparticles is Quadratic model. **Table 4.12** below shows the ANOVA analysis of the suggested linear model.

**Table 4.11 ANOVA Table for Response Surface linear Model**

| | Sum of | | Mean | F | p-value | |
|---|---|---|---|---|---|---|
| Source | Squares | df | Square | Value | Prob > F | |
| Model | 195.87 | 9 | 21.76 | 12.25 | 0.0016 | significant |
| *A-Polymer Concentration* | *36.89* | *1* | *36.89* | *20.77* | *0.0026* | |
| *B-Drug Concentration* | *75.95* | *1* | *75.95* | *42.76* | *0.0003* | |
| *C-Ratio of Solvent to Water* | *0.24* | *1* | *0.24* | *0.14* | *0.7232* | |
| *AB* | *15.29* | *1* | *15.29* | *8.61* | *0.0219* | |
| *AC* | *0.18* | *1* | *0.18* | *0.099* | *0.7618* | |
| *BC* | *0.051* | *1* | *0.051* | *0.029* | *0.8707* | |
| *A^2* | *8.55* | *1* | *8.55* | *4.81* | *0.0643* | |
| *B^2* | *23.40* | *1* | *23.40* | *13.17* | *0.0084* | |
| *C^2* | *28.73* | *1* | *28.73* | *16.18* | *0.0050* | |
| Residual | 12.43 | 7 | 1.78 | | | |
| *Lack of Fit* | *3.93* | *3* | *1.31* | *0.62* | *0.6404* | *not significant* |
| *Pure Error* | *8.51* | *4* | *2.13* | | | |
| Cor Total | 208.30 | 16 | | | | |

The Model F-value of 12.25 implies the model is significant. There is only a 0.16% chance that an F-value this large could occur due to noise. Values of "Prob > F" less than 0.0500 indicate model terms are significant. In this case A, B, AB, B^2, C^2 are significant model terms. Values greater than 0.1000 indicate the model terms are not significant. If there are many insignificant model terms (not counting those required to support hierarchy), model reduction may improve your model. The "Lack of Fit F-value" of 0.62 implies the Lack of Fit is not significant relative to the pure error. There is a 64.04% chance that a "Lack of Fit F-value" this large could occur due to noise. Non-significant lack of fit is good -- we want the model to fit.

**Table 4.12 Summary of ANOVA results for Quadratic Model**

| | | | |
|---|---|---|---|
| Std. Dev. | 1.33 | R-Squared | 0.9403 |
| Mean | 4.66 | Adj R-Squared | 0.8636 |
| C.V. % | 28.58 | Pred R-Squared | 0.6346 |
| PRESS | 76.11 | Adeq Precision | 11.264 |

The "Pred R-Squared" of 0.6346 is not as close to the "Adj R-Squared" of 0.8636 as one might normally expect; i.e. the difference is more than 0.2. This may indicate a large block effect or a possible problem with your model and/or data. Things to consider are

model reduction, response transformation, outliers, etc. All empirical models should be tested by doing confirmation runs. "Adeq Precision" measures the signal to noise ratio. A ratio greater than 4 is desirable. Your ratio of 11.264 indicates an adequate signal. This model can be used to navigate the design space.

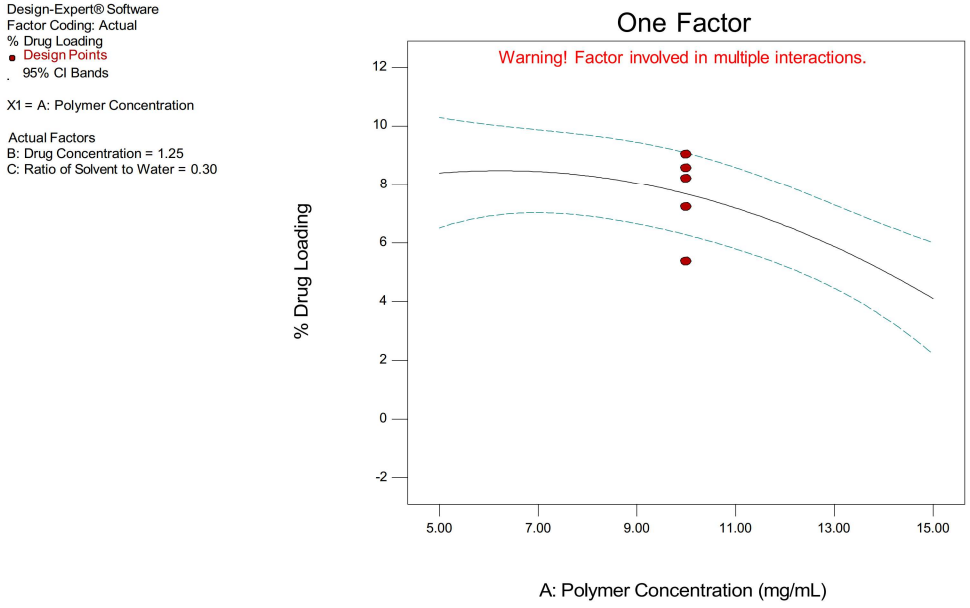


**Figure 4.14 Effect of polymer concentration on % drug loading**

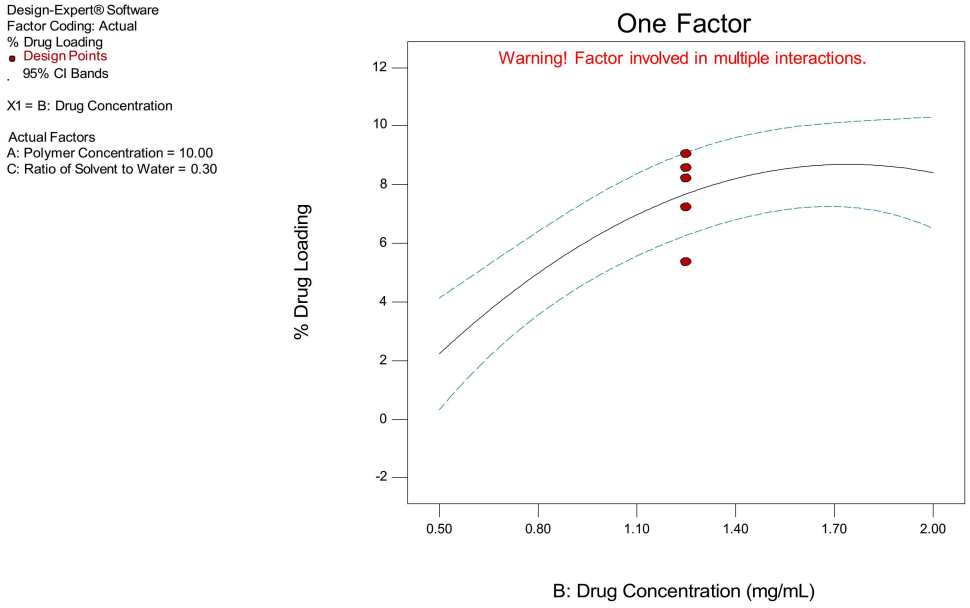


**Figure 4.15 Effect of drug concentration on % drug loading**

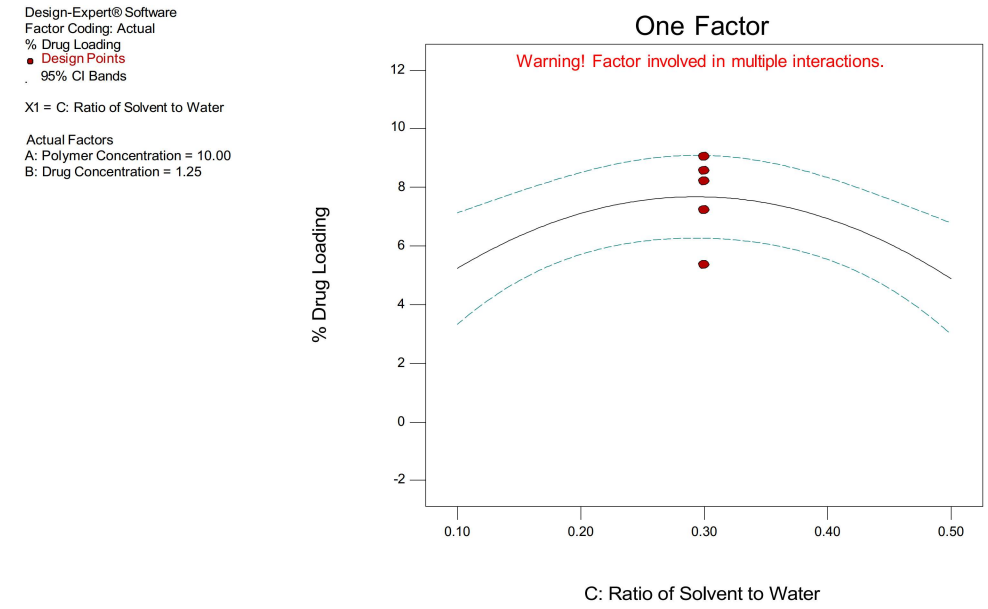


**Figure 4.16 Effect of ratio of solvent to water on % drug loading**

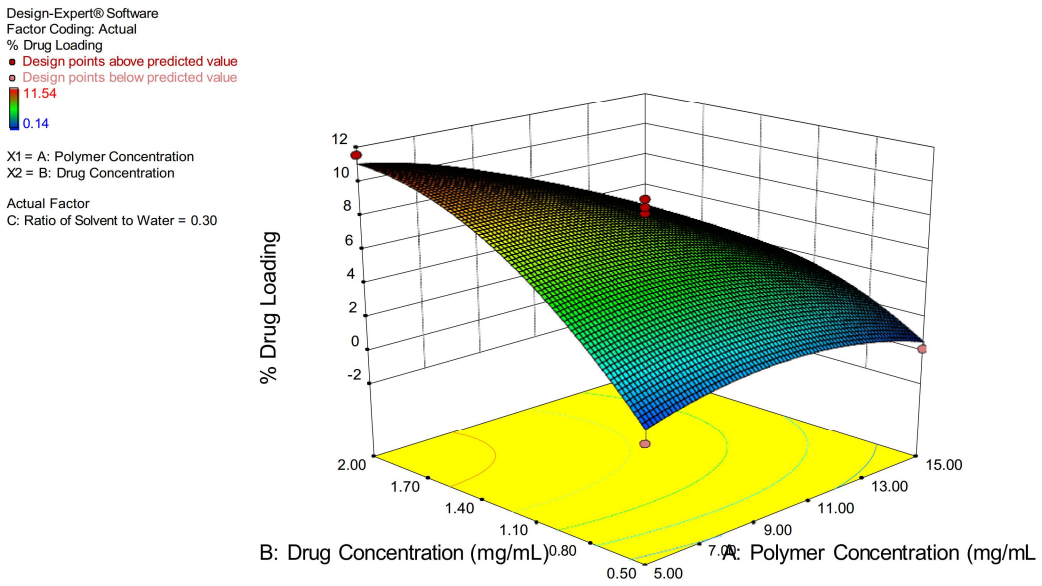


**Figure 4.17 Response surface showing combined effect of drug concentration and polymer concentration on % drug loading**

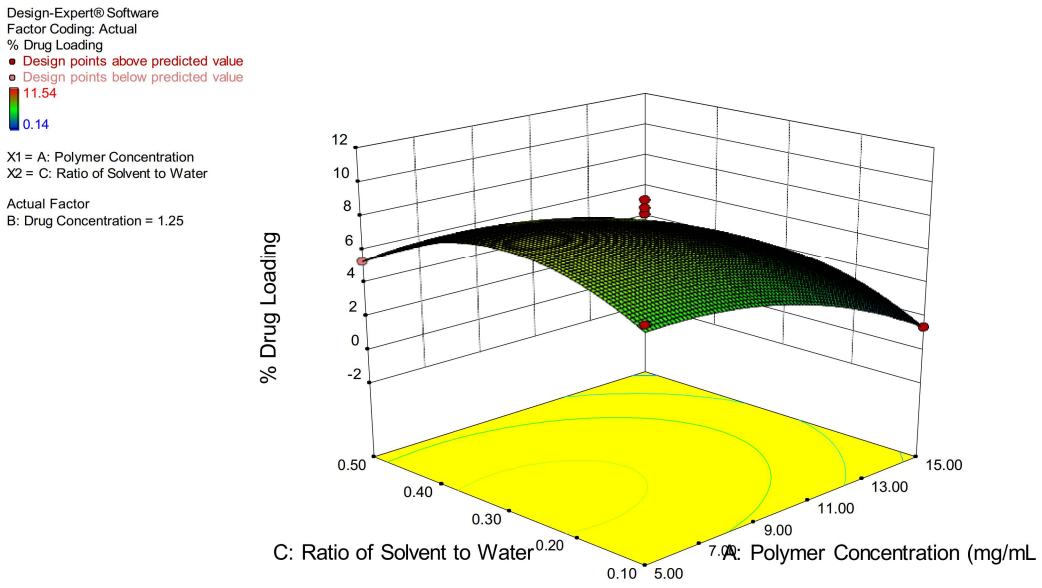


**Figure 4.18 Response surface showing combined effect of Ratio of Solvent to Water and polymer concentration on % drug loading**

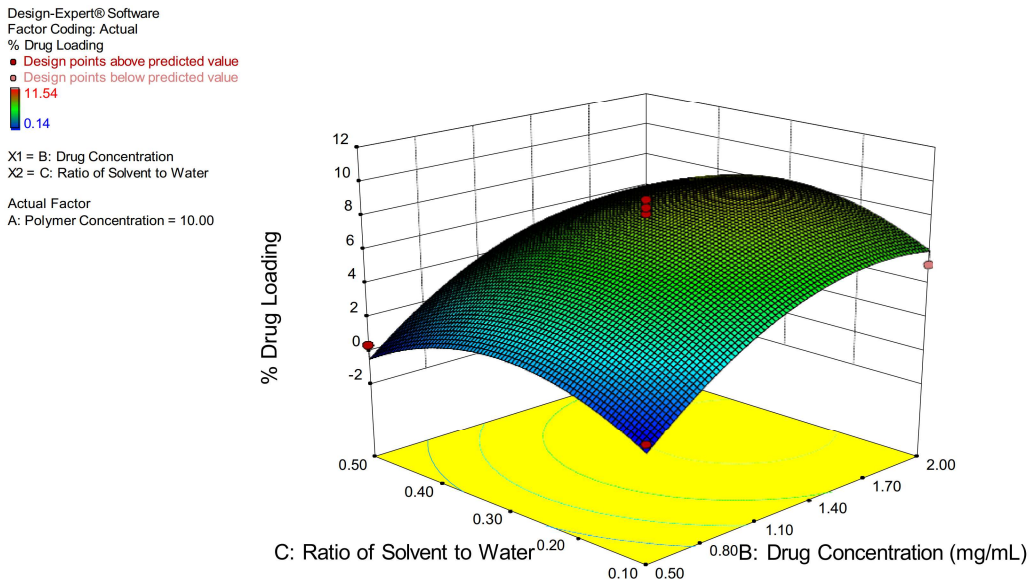


**Figure 4.19 Response surface showing combined effect of Ratio of Solvent to Water and drug concentration on % drug loading**

**Predicted response at any point of the plot can be represented by the following equation:**

% Drug Loading =

-17.20019

+1.29897 * Polymer Concentration

+20.02333 * Drug Concentration

+37.15250 * Ratio of Solvent to Water

-0.52133 * Polymer Concentration * Drug Concentration

+0.21000 * Polymer Concentration * Ratio of Solvent to Water

-0.75000 * Drug Concentration * Ratio of Solvent to Water

-0.056990 * Polymer Concentration^2

-4.19067 * Drug Concentration^2

-65.30625 * Ratio of Solvent to Water^2

***iv. Selection of Optimized Batch:***

Constraints applied to select the best formulation parameters based on the % Drug Loading, particle size and PDI are shown in the following **Table 4.13**.

**Table 4.13 Constraints Applied for Selection of Optimized Batch**

| Name | Goal | Lower Limit | Upper Limit |
|---|---|---|---|
| Particle Size | Minimum | 150.0 | 225.0 |
| % Drug Loading | Maximum | 8.0 | 12.0 |
| PDI | Minimum | 0.01 | 0.99 |

***v. Point Prediction and Confirmation:***

Confirmation of the response was done by carrying out the experiment using the selected factor values in triplicate. The **Table 4.14** shows and confirms that experimental and predicted values are in good agreement concluding the suitability of the selected model for optimization.

**Table 4.14 Experimental Confirmation of the Predicted Responses***

| Response | Predicted | Experimental |
|---|---|---|
| Particle Size | 183.82 | 187.54 |
| PDI | 0.202 | 0.190 |
| % Drug Loading | 10.95 | 11.55 |

*Experiments were performed in triplicate.

Nanoparticulate batch optimized so was used for further modification of surface using Cetuximab mAb.

### 4.8 Lyophilization and optimization of cryoprotectant concentration

The nanoparticle dispersions have thermodynamic instability upon storage and lead to the formation of aggregates. Freeze-drying/lyophilization is one of the best-known methods to recover nanoparticles in the dried form and suitably redisperse them at the time of administration. To the suspension of the nanoparticles different cryoprotectants like sucrose, mannitol and trehalose were added in different concentrations at nanoparticle (NP): cryoprotectant (CP) ratio of 1:1, 1:2 and 1:3 before freeze-drying.(24,46,47)

### 4.9 Antibody conjugation of nanoparticles

The surface modification of Docetaxel loaded PLGA nanoparticles with antibody Cetuximab was achieved in two steps using carbodiimide coupling method. This active ester method yields stable amide bonds. As a prerequisite, the polymer has to contain free carboxyl groups at the surface as represented by the H-type of PLGA which are activated by carbodiimide/N-hydroxysuccinimide.(30,48–50) In contrast to the activation of carboxyls with only carbodiimide, the presence of N-hydroxysuccinimide yields Nhydroxysuccinimide esters as stable intermediates which rather acylate amino groups of proteins than to be subject of hydrolysis in aqueous medium. Activation pH, reaction temperature, activation time and amount of activating agents (EDC-HCl/NHS) were optimized to achieve minimum particle size and maximum conjugation efficiency.

Briefly, in first step, to the lyophilized drug containing nanoparticles dispersed in phosphate buffer pH adjusted to 5.0, using potassium dihydrogen phosphate was added freshly prepared aqueous solution of EDC with continuous stirring on a magnetic stirrer followed by an equimolar freshly prepared aqueous solution of NHS after half an hour. Then, the mixture was allowed to stir on a magnetic stirrer for 30 minutes more. Then the activated nanoparticles were recovered by centrifuging at 50000 rpm for 15 min, washed with distilled water and suspended in phosphate buffer pH 7.4. The temperature was maintained below 15°C throughout the conjugation (45,49).

In the second step, to the dispersion of activated nanoparticles was added solution of cetuximab in phosphate buffer pH 7.4. The mixture was stirred for one hour, centrifuged at 50000 rpm for 15 minutes at 15°C to separate Cetuximab conjugated nanoparticles and washed twice with phosphate-buffered saline (PBS) 7.4 to remove unreacted reagents and Cetuximab. The temperature was maintained below 15 °C throughout the

conjugation. To saturate the free coupling sites 1.0 ml of 20 % glycine solution in 20mM HEPES/NaOH buffer, pH 7.4 was added and incubated for 1 hr. Finally, the particles were washed with distilled water and lyophilized for 24hrs .

### 4.9.1 Estimation of conjugation efficiency of antibody to the nanoparticles (Determination of mAb on the surface of nanoparticles)

The concentration of proteins can be estimated using various methods. For estimating the total protein in a complex protein mixture, one can use dyes that exhibit changes in their spectral properties on binding to the proteins. Bradford is one such dye-based assay for protein concentration estimation. (51,52)

The principle underlying Bradford assay is the binding of the Coomassie Blue G250 dye to proteins.

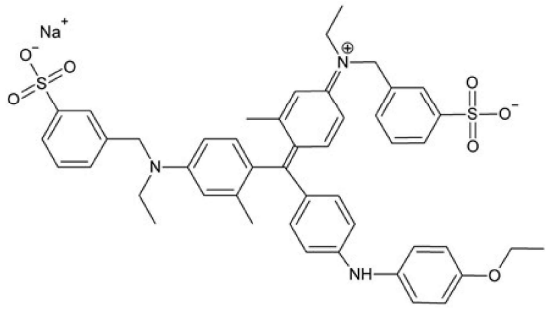


**Figure 4.20 Chemical structure of Coomassie Blue**

Free Coomassie Blue G250 can exist in four different ionization states with pKα1, pKα2, and pKα3 of 1.15, 1.82, and 12.4. At pH 0, both the sulfate groups are negatively charged and all three nitrogen are positively charged giving the dye +1 net charge (the red form of the dye). Around pH 1.5, the neutral green form of the dye predominates. At neutral pH, the dye has a net charge of +1 (the blue form of the dye). The red, green, and blue forms of the dye absorb visible radiation with absorption maxima at 470, 650, and 590 nm, respectively. It is the anionic form of the dye that binds to the protein. Binding of the blue form of Coomassie Blue G250 with proteins causes red-shift in its absorption spectrum; the absorption maximum shifts from 590 to 620 nm. It, therefore, looks sensible to record the absorption at 620 nm. The absorbance, however, is recorded at 595 nm to avoid any contribution from the green form of the dye. The dye binds more readily to the cationic residues, lysine and arginine. This implies that the response of the assay

would depend on the amino acid composition of protein, the major drawback of the assay. The original assay developed by Bradford shows such variation between different proteins. Several modifications have been introduced into the assay to overcome this drawback; the modified assays, however, are more susceptible to interference by other chemicals than the original assay. The original Bradford assay, therefore, remains the most convenient and widely used method (53).

The Bradford method with Coomassie dye was used. 300 µl of Coomassie Plus reagent was added to 10 µl of dispersion of nanoparticles, either mAb-conjugated or non-conjugated, and after 10 min of incubation, the absorbance was measured at 595 nm. The results were compared to a standard curve of BSA solution in the concentration range from 10 µg/ml to 750 µg/ml.

The % conjugation efficiency was calculated as follows:

$$\%\ \text{conjugation efficiency} = \frac{\text{Cetuximab added} - \text{unreacted Cetuximab}}{\text{Cetuximab added}} X100$$

**4.9.2 Optimization for conjugation of Cetuximab in Docetaxel loaded Nanoparticles**

**4.9.2.1 Influence of pH on conjugation efficiency**

The effect of pH on the conjugation efficiency of Cetuximab to nanoparticles was checked by varying the pH during activation, i.e. step 1, between 5 to7 keeping pH during antibody conjugation, i.e. step 2, at 7.4 to avoid any protein denaturation. The weight of Cetuximab to weight of nanoparticles ratio was taken as 1:10, concentration of EDC and NHS as 7 µM, activation time as 1 hr (first step) and reaction temperature as 15°C.

**4.9.2.2 Influence of temperature on conjugation efficiency**

The effect of temperature on Cetuximab conjugation to nanoparticles was tested by varying the reaction temperature (of first step and second step) between 15-25 °C and the results are recorded in table 4.18. The weight of Cetuximab to weight of nanoparticles ratio was taken as 1:10, concentration of EDC and NHS as 7 µM, activation time as 1 hr (first step) and activation pH as 5 for step 1 and 7.4 for step 2.

**4.9.2.3 Influence of amount of activating agent**

The influence of the amount of activating agent (EDC/NHS concentration) on conjugation efficiency of Cetuximab to nanoparticles was assessed by varying the amount of EDC/NHS, keeping the weight of Cetuximab to weight of nanoparticles ratio

as 1:10, pH as 5 during activation and 7.4 during conjugation, activation time as 1 hr (first step) and reaction temperature as 15°C.

**4.9.2.4 Influence of reaction time**

The influence of reaction time (activation and conjugation time i.e. time for step 1 + step 2) on conjugation efficiency of Cetuximab to nanoparticles was assessed by varying the PLGA nanoparticles activation time, keeping the weight of Cetuximab to weight of nanoparticles ratio as 1:10; pH as 5 during activation and 7.4 during conjugation, concentration of EDC-HCl and NHS as 7.8 μM and reaction temperature as 15°C.

**4.9.2.5 Influence of amount of antibody**

The effect of amount of Cetuximab antibody on conjugation efficiency and particle size was checked by varying the amount of antibody added to the activated nanoparticles. The concentration of EDC and NHS was taken as 7 μM, activation pH as 5 for first step and 7.4 for second step and reaction temperature as 15°C.

**4.9.3 Characterization of immunonanoparticles**

**4.9.3.1 Particle size and zeta potential**

A 2.0 mg sample of lyophilized drug containing nanoparticles, unconjugated and antibody conjugated, was suspended in distilled water, and the particle size and zeta potential were measured using the principle of laser light scattering with zeta sizer.

**4.9.3.3 In-vitro drug release**

The invitro drug release of the Docetaxel nanoparticles was performed in pH 1.2 Acid, phosphate-buffer pH 6.8 and pH 7.4 at 37°C using rotating bottle apparatus. Nanoparticles equivalent to 1mg drug were suspended in 10 ml of release media in screw capped tubes, which were placed in horizontal shaker bath maintained at 37°C and shaken at 60 rpm. At specific time intervals following incubation samples were taken out and centrifuged at 50000 rpm for 30 min. The residue was collected and dissolved in acetonitrile, diluted suitably and analyzed by UV spectrophotometer for respective drug. (8,54–56) The amount of the drug released was calculated using the following equation. The release of drug from the unconjugated and conjugated nanoparticles is tabulated in table 4.23 and shown graphically in figure 4.15.

$$\%\,\text{drug released} = \frac{\text{drug added in formulation - amount of drug in nanoparticles}}{\text{drug added in formulation}} X100$$

### 4.9.5 Determination of residual Acetone in nanoparticles

As per USP, residual solvents are tested under General Chapter <467> "Organic Volatile Impurities." (57)

## 4.10 Results and Discussion

### 4.10.1 Lyophilization and optimization of cryoprotectant concentration

Freeze-drying has been the most utilized drying method for nanoparticle system. Since, freeze-drying is a highly stressful process for nanoparticles, addition of cryoprotectants become essential. For nanoparticles carbohydrates have been perceived to be suitable freeze-drying protectants.(46) There are considerable differences in the cryoprotective abilities of different carbohydrates. The optimized batch of nanoparticles was lyophilized using sucrose, mannitol and trehalose (at 1:1, 1:2 and 1:3 nanoparticle to cryoprotectant) to select suitable cryoprotectant and its concentration.(24,46) The redispersibility of the freeze-dried formulations and particle size of the nanoparticles before and after freeze-drying were evaluated and recorded in **Table 4.16.**

**Table 4.16: Effect of different cryoprotectants on the particle size and redispersion of NG nanoparticles**

| Type of cryoprotectant | NP: CP ratio | Particle size (nm) | | Sf/Si | Redispersion |
|---|---|---|---|---|---|
| | | Before Lyophilization Si | After Lyophilization Sf | | |
| Initial | 1 : 0 | 165.23 ± 6.51 | NA | NA | NA |
| Sucrose | 1 : 1 | -- | 538.65 | 3.26 | Poor redispersibility |
| Sucrose | 1 : 2 | -- | 418.03 | 2.53 | Poor redispersibility |
| Sucrose | 1 : 3 | -- | 375.07 | 2.27 | Poor redispersibility |
| Trehalose | 1 : 1 | -- | 287.50 | 1.74 | Moderate redispersibility |
| Trehalose | 1 : 2 | -- | 224.71 | 1.36 | Easy redispersibility |
| Trehalose | 1 : 3 | -- | 178.45 | 1.08 | Easy redispersibility |
| Mannitol | 1 : 1 | -- | 383.33 | 2.32 | Moderate redispersibility |
| Mannitol | 1 : 2 | -- | 335.42 | 2.03 | Moderate redispersibility |
| Mannitol | 1 : 3 | -- | 194.97 | 1.18 | Moderate redispersibility |

With the use of sucrose as cryoprotectant, the cake formed after lyophilization was found to be of condensed and collapsed structure. Hence, the redispersibility of nanoparticles was poor and was only possible with sonication. For the different ratios of 1:1, 1:2 and

1:3 nanoparticle to cryoprotectant, as shown in table 4.16, increased significantly after lyophilization.(24,58,47,59) The Sf/Si values were 3.26, 2.53 and 2.27 with 1:1, 1:2 and 1:3 nanoparticle to sucrose respectively. The increase in the particle size could have been due to the cohesive nature of the cryoprotectant. Further, it was observed that the lyophilized nanoparticles with sucrose had tendency to absorb moisture quickly. While, with mannitol the lyophilized product was fluffy and snow like voluminous cake. Also, the nanoparticle formulation showed free flowing.(24,46,59) However, the redispersibility of nanoparticles was difficult and possible only after vigorous shaking. The particle size, recorded in table 4.16, increased significantly after lyophilization than the initial. The Sf/Si values were 2.32, 2.03 and 1.18 with 1:1, 1:2 and 1:3 nanoparticle to mannitol respectively. This may be due to the low solubility of mannitol in water (0.18 parts of mannitol soluble in 1 part of water). With trehalose also, the lyophilized nanoparticles formed fluffy and snow like voluminous cake. With trehalose as cryoprotectant, the lyophilized nanoparticles were redispersed easily and the increase in particle size was not significant as indicated by Sf/Si values 1.7, 1.36, and 1.08 for 1:1, 1:2 and 1:3 nanoparticle to trehalose respectively (table 4.16).(58,59) The redispersion of the nanoparticles depends on the hydrophilicity of the surface. The easy redispersibility could be probably due to the higher solubility of trehalose in water (0.7 parts in 1 part of water). The cryoprotective effect may be attributed to the ability of trehalose to form a glassy amorphous matrix around the particles, preventing the particles from sticking together during removal of water. In addition, the property of the Tyndall effect observed with nanoparticles was retained after redispersion of the nanoparticles lyophilized using trehalose. Furthermore, trehalose, a non-reducing disaccharide of glucose, has previously demonstrated satisfactory cryoprotective effects for pharmaceutical and biological materials. Therefore, trehalose at a ratio of 1:4 (nanoparticles: trehalose) was used as cryoprotectant for lyophilization of optimized batch of nanoparticles for further studies.

**4.10.2 Antibody conjugation to nanoparticles**

The activation pH, reaction temperature, activation time, amount of activating agents (EDC/NHS) and Cetuximab to NPs ratio were optimized to achieve minimum particle size and maximum conjugation efficiency.

The activation pH was varied between pH 5-7 and at acidic pH 5 highest conjugation efficiency was observed with a decrease in %EE which may be due to hydrolysis of PLGA at this pH (**Table 4.17**).

**Table 4.17: Optimization of antibody-conjugation activation pH**

| pH | Conjugation efficiency (%w/w) | Mean particle size (nm) | %EE (%w/w) |
|---|---|---|---|
| 4 | 28.95 ± 1.2 | 165.24 ± 3.5 | 57.5 ± 1.8 |
| 5 | 36.54 ± 1.5 | 168.55 ± 5.7 | 55.24 ± 2.7 |
| 6 | 27.72 ± 1.7 | 164.51 ± 6.8 | 56.84 ± 1.5 |
| 7 | 12.68 ± 2.1 | 162.84 ± 3.7 | 54.62 ± 2.2 |

Antibody-conjugation is generally used as a carboxyl activating agent in the pH range of 4.0-6.0 and hence a low conjugation efficiency was observed at pH 7 followed by at pH 6. Hence, taking into account the conjugation efficiency and %EE, the activation pH was optimized as 5 for nanoparticle activation followed by antibody conjugation effected at pH 7.4 to avoid denaturation of protein at lower pH. It was observed that the activation pH did not significantly affect the mean particle size of antibody-conjugated nanoparticles.

The effect of temperature on antibody conjugation to nanoparticles was also evaluated and the results are recorded in **Table 4.18.**

**Table 4.18 Optimization of antibody conjugation reaction temperature**

| Temperature | Conjugation efficiency (%w/w) | Mean particle size (nm) | %EE (%w/w) |
|---|---|---|---|
| 15°C | 35.87 ± 3.2 | 172.54 ± 5.7 | 54.62 ± 2.2 |
| 20°C | 24.44 ± 2.4 | 168.21 ± 4.1 | 55.24 ± 2.7 |
| 25°C | 16.65 ± 2.8 | 159.53 ± 7.2 | 56.25 ± 1.9 |

At a reaction temperature of 25°C both the conjugation efficiency and %EE were observed to be the lowest which may be attributed to low glass transition temperature of PLGA resulting in increased drug leaching from nanoparticles and availability of less surface carboxyl group to effect conjugation. The same may explain for a low conjugation efficiency and %EE at 20°C. In addition, carbodiimide coupling has been reported to be efficient at room temperature. While both conjugation efficiency and %EE were observed to be high at a temperature of 15°C and hence, was optimized as reaction temperature.

The effect of the amount of activating agent (EDC/NHS concentration) on conjugation efficiency of antibody to nanoparticles was assessed and the results recorded in **Table 4.19.**

**Table 4.19 Optimization of amount of activating agent**

| Amount of EDC/NHS (μM) | Conjugation efficiency (%w/w) | Mean particle size (nm) | %EE (%w/w) |
|---|---|---|---|
| 6.0 | 27.65 ± 2.2 | 171.54 ± 6.9 | 54.52 ± 1.7 |
| 7.5 | 38.50 ± 2.8 | 164.14 ± 5.7 | 59.14 ± 2.3 |
| 9.0 | 39.77 ± 3.4 | 163.57 ± 6.1 | 58.62 ± 3.1 |

It was observed that increasing the concentration of activating agent from 6.0 to 9.0 μM there was an increase in conjugation efficiency from 27.65 ± 2.2% to 39.77 ± 3.4% with no appreciable effect on mean particle size or %EE of antibody conjugated nanoparticles. While, there was no significant increase in antibody conjugation efficiencies of nanoparticles with increase in EDC/NHS concentration from 6.0 to 9.0 μM μM indicating nanoparticle surface saturation with unavailability of surface carboxyl groups for more antibody attachment.(30)

The influence of reaction time (activation and conjugation time) on conjugation efficiency of Cetuximab to nanoparticles was also checked and the results are recorded in **Table 4.20.**

**Table 4.20 Optimization of antibody conjugation reaction time**

| Reaction time | Conjugation efficiency (%w/w) | Mean particle size (nm) | %EE (%w/w) |
|---|---|---|---|
| 1 hours | 24.36 ± 2.5 | 168.59 ± 5.8 | 61.21 ± 2.8 |
| 2 hours | 37. 77 ± 1.9 | 165.54 ± 4.8 | 55.22 ± 2.5 |
| 3 hours | 38.50 ± 1.5 | 162.17 ± 5.2 | 56.82 ± 2.7 |

The conjugation efficiency of antibody to nanoparticles was observed to be significantly low with a reaction time of 1 hr (half an hour each for activation and conjugation) with no significant effect on particle size and %EE indicating the time to be insufficient to achieve maximum antibody conjugation. However, there was no significant increase in antibody conjugation, mean particle size and %EE with increase in reaction time from 2 to 3 hr. Thus, the reaction time was standardized as 2 hr.

The amount of antibody (Cetuximab) was varied from 10µg to 500µg (**Table 4.21**).

**Table 4.21 Optimization of amount of antibody**

| Antibody amount (Antibody:NPs ratio) | Conjugation efficiency (%w/w) | Mean particle size (nm) | %EE (%w/w) |
|---|---|---|---|
| 10 µg (1:50) | 19.97 ± 2.8 | 165.16 ± 7.4 | 58.84 ± 3.1 |
| 20 µg (1:25) | 25.88 ± 2.4 | 171.28 ± 8.7 | 61.23 ± 1.7 |
| 500 µg (1:1) | 39.59 ± 2.7 | 168.55 ± 7.9 | 63.55 ± 2.5 |

For all the three drug nanoparticles, with increase in the amount of antibody the conjugation efficiency increased with no significant increase in particle size. This is because by increasing the antibody concentration from 10µg to 500µg no surface saturation was observed for PLGA nanoparticles with respect to the antibody attached as it has not been used in molar ratios.

### 4.10.3 Particle size, zeta potential and drug entrapment efficiency

The particle size, zeta potential and drug entrapment efficiency (%EE) for drug loaded unconjugated nanoparticles and antibody conjugated drug loaded nanoparticles are measured and the particle size and zeta potential for the nanoparticles are shown graphically in **Figure 4.21**.

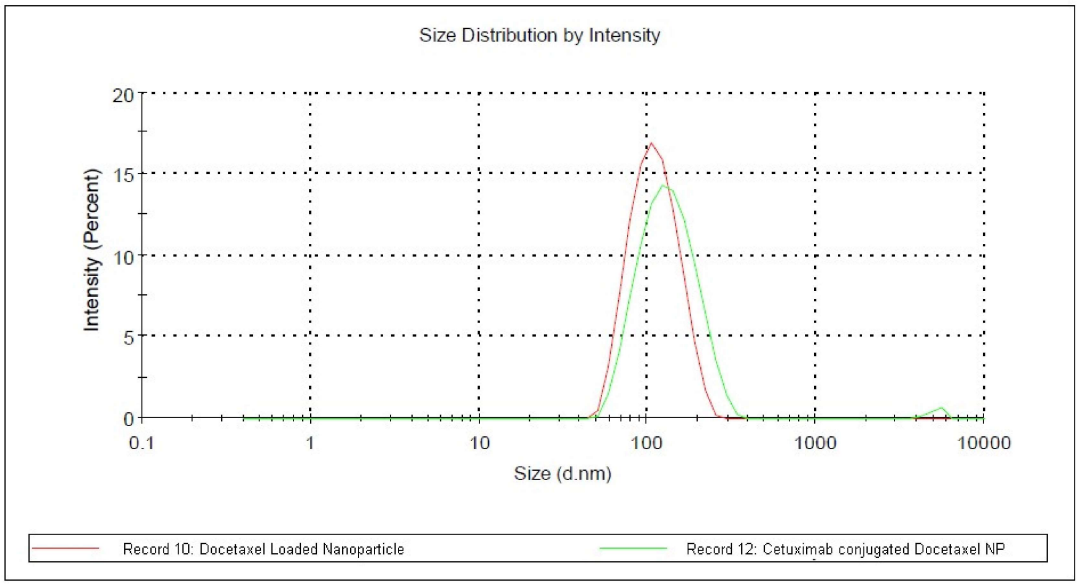


**Figure 4.21 Particle size distributions**

Increase in the particle size after antibody conjugation may be due to antibody conjugation to the surface of unconjugated nanoparticles. While, the increase in zeta potential may be due to screening of the negative charge because of the antibody conjugated to the nanoparticle surface.(8,17,24,60,61) In addition, the decrease in %EE may be explained by the accelerated leaching of the drug from the nanoparticles being subjected to different pH conditions during antibody conjugation.

The particle size plays a vital role in in vivo systemic circulation, tissue distribution and its clearance from the central compartment. It has been reported that tumor possess impaired lymphatic drainage and interstitial spaces.

### 4.10.4 In-vitro drug release

The release of the drug from PLGA is by the degradation of polymer by hydrolysis of its ester linkages in the presence of water. In general the mechanism by which active agent is released from a delivery vehicle is a combination of diffusion of the active agent from the polymer matrices, bulk erosion of the polymer, swelling and degradation of the polymer.(62) The degradation of PLGA is slow, therefore the release of the drugs from the nanoparticles may depend on drug diffusion and PLGA surface and bulk erosion or swelling. The results of in vitro drug release profiles for the drug NPs are shown graphically in **Figure 4.22**.

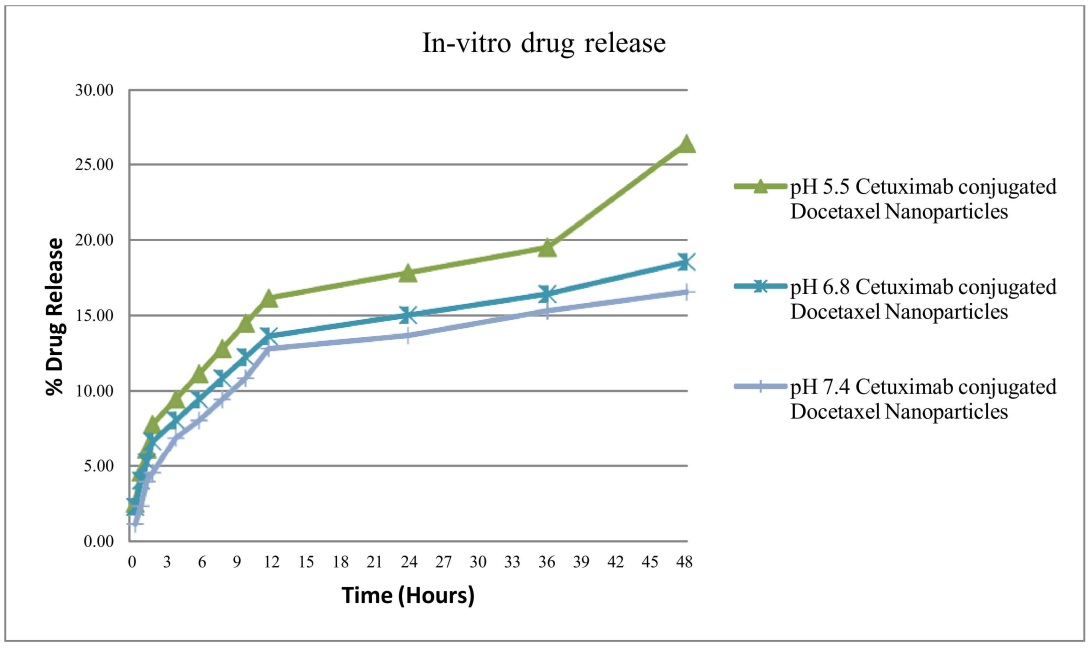


**Figure 4.22 In-vitro drug release from cetuximab conjugated Docetaxel Nanoparticles**

For the entire drug loaded unconjugated nanoparticles there was an initial burst release for 12 hrs and then there was a lag phase and continuous zero order drug release in 48 hours. This high initial burst from unconjugated nanoparticles can be attributed to the immediate dissociation and dissolution of drug adhered on the surface and located near the surface of the nanoparticles.(38,60) After that, in lag phase, the release is mainly due to the erosion of the polymer matrix and further diffusion of drug molecules through the polymeric matrix of the nanoparticles. The matrix material would require time to erode in the aqueous environment than the release mechanisms of surface release, resulting in the prolonged release.

The burst effect was absent in antibody conjugated drug nanoparticles and the release was following zero order kinetics. The absence of burst release with antibody-conjugated nanoparticles may be due to absence of drug on the surface of conjugated nanoparticles.

**4.10.5 Determination of residual acetone in nanoparticles**

Residual acetone was found to be within the permissible limit for both unconjugated and antibody-conjugated nanoparticles. Residual acetone of antibody-conjugated nanoparticles was less than the unconjugated nanoparticles and can be due to the evaporation/washing of surface acetone during conjugation process.

Reference List

1. Bissery MC, Gu??nard D, Gu??ritte-Voegelein F, Lavelle F. Experimental antitumor activity of taxotere (RP 56976, NSC 628503), a taxol analogue. Cancer Res. 1991;51(18):4845–52.
2. Clarke SJ, Rivory LP. Clinical pharmacokinetics of docetaxel. Clin Pharmacokinet [Internet]. 1999;36(2):99–114. Available from: http://www.ncbi.nlm.nih.gov/pubmed/10092957
3. Cortes JE, Pazdur R. Docetaxel. J Clin Oncol [Internet]. 1995;13(10):2643–55. Available from: http://www.ncbi.nlm.nih.gov/pubmed/7595719
4. Baker SD, Sparreboom A, Verweij J. Clinical pharmacokinetics of docetaxel: Recent developments. Clinical Pharmacokinetics. 2006. p. 235–52.
5. Fukumori Y, Ichikawa H. Nanoparticles for cancer therapy and diagnosis. Adv Powder Technol [Internet]. 2006;17(1):1–28. Available from: http://www.sciencedirect.com/science/article/pii/S0921883108607888
6. Wang T, Bai J, Jiang X, Nienhaus GU. Cellular uptake of nanoparticles by membrane penetration: A study combining confocal microscopy with FTIR spectroelectrochemistry. ACS Nano. 2012;6(2):1251–9.
7. Sun T, Zhang YS, Pang B, Hyun DC, Yang M, Xia Y. Engineered nanoparticles for drug delivery in cancer therapy. Angew Chem Int Ed Engl. 2014;53(46):12320–64.
8. Jain A, Thakur K, Sharma G, Kush P, Jain UK. Fabrication, characterization and cytotoxicity studies of ionically cross-linked docetaxel loaded chitosan nanoparticles. Carbohydr Polym [Internet]. 2016 Feb [cited 2015 Nov 18];137:65–74. Available from: http://www.sciencedirect.com/science/article/pii/S0144861715009923
9. Tahara K, Sakai T, Yamamoto H, Takeuchi H, Hirashima N, Kawashima Y. Improved cellular uptake of chitosan-modified PLGA nanospheres by A549 cells. Int J Pharm [Internet]. 2009 Dec 1 [cited 2016 Feb 13];382(1-2):198–204. Available from: http://www.sciencedirect.com/science/article/pii/S0378517309004955
10. Muthu M. Nanoparticles based on PLGA and its co-polymer: An overview. Asian J Pharm. 2009;3(4):266.
11. Lu JM, Wang X, Marin-Muller C, Wang H, Lin PH, Yao Q, et al. Current

advances in research and clinical applications of PLGA-based nanotechnology. Expert Rev Mol Diagn [Internet]. 2009;9(4):325–41. Available from: http://www.ncbi.nlm.nih.gov/pubmed/19435455

12. Cheng J, Teply BA, Sherifi I, Sung J, Luther G, Gu FX, et al. Formulation of functionalized PLGA – PEG nanoparticles for in vivo targeted drug delivery. Biomaterials. 2007;28:869–76.
13. Storm G, Belliot SO, Daemen T, Lasic DD. Surface modification of nanoparticles to oppose uptake by the mononuclear phagocyte system. Adv Drug Deliv Rev [Internet]. 1995 Oct [cited 2015 Dec 14];17(1):31–48. Available from: http://www.sciencedirect.com/science/article/pii/0169409X9500039A
14. Hickey JW, Santos JL, Williford J-M, Mao H-Q. Control of polymeric nanoparticle size to improve therapeutic delivery. J Control Release [Internet]. 2015 Dec 10 [cited 2016 Jan 17];219:536–47. Available from: http://www.sciencedirect.com/science/article/pii/S0168365915301759
15. Panagi Z, Beletsi A, Evangelatos G, Livaniou E, Ithakissios D., Avgoustakis K. Effect of dose on the biodistribution and pharmacokinetics of PLGA and PLGA–mPEG nanoparticles. Int J Pharm [Internet]. 2001 Jun [cited 2016 Feb 13];221(1-2):143–52. Available from: http://www.sciencedirect.com/science/article/pii/S0378517301006767
16. Peter Christoper G V, Vijaya Raghavan C, Siddharth K, Siva Selva Kumar M, Hari Prasad R. Formulation and optimization of coated PLGA - Zidovudine nanoparticles using factorial design and in vitro in vivo evaluations to determine brain targeting efficiency. Saudi Pharm J SPJ Off Publ Saudi Pharm Soc [Internet]. 2014 Apr [cited 2016 Feb 13];22(2):133–40. Available from: http://www.sciencedirect.com/science/article/pii/S1319016413000406
17. Akl MA, Kartal-Hodzic A, Oksanen T, Ismael HR, Afouna MM, Yliperttula M, et al. Factorial design formulation optimization and in vitro characterization of curcumin-loaded PLGA nanoparticles for colon delivery. J Drug Deliv Sci Technol [Internet]. 2016 Jan [cited 2016 Jan 20];32:10–20. Available from: http://www.sciencedirect.com/science/article/pii/S1773224716300065
18. Mattos AC de, Altmeyer C, Tominaga T, Khalil NM, Mainardes RM. Polymeric nanoparticles for oral delivery of 5-fluorouracil: Formulation optimization, cytotoxicity assay and pre-clinical pharmacokinetics study. Eur J Pharm Sci

[Internet]. 2016 Jan 14 [cited 2016 Jan 25];84:83–91. Available from: http://www.sciencedirect.com/science/article/pii/S0928098716300124

19. Dhas NL, Ige PP, Kudarha RR. Design, optimization and in-vitro study of folic acid conjugated-chitosan functionalized PLGA nanoparticle for delivery of bicalutamide in prostate cancer. Powder Technol [Internet]. 2015 Oct [cited 2016 Feb 13];283:234–45. Available from: http://www.sciencedirect.com/science/article/pii/S0032591015003381
20. Vial J, Cohen M, Sassiat P, Thiébaut D. Pharmaceutical quality of docetaxel generics versus originator drug product: a comparative analysis. Curr Med Res Opin. 2008;24(7):2019–33.
21. Sangshetti JN, Deshpande M, Zaheer Z, Shinde DB, Arote R. Quality by design approach: Regulatory need. Arab J Chem [Internet]. 2014 Feb [cited 2015 Dec 24]; Available from: http://www.sciencedirect.com/science/article/pii/S1878535214000288
22. Yerlikaya F, Ozgen A, Vural I, Guven O, Karaagaoglu E, Khan MA, et al. Development and evaluation of paclitaxel nanoparticles using a quality-by-design approach. J Pharm Sci [Internet]. 2013 Oct [cited 2016 Feb 24];102(10):3748–61. Available from: http://www.sciencedirect.com/science/article/pii/S0022354915308935
23. Curić A, Reul R, Möschwitzer J, Fricker G. Formulation optimization of itraconazole loaded PEGylated liposomes for parenteral administration by using design of experiments. Int J Pharm [Internet]. 2013 May 1 [cited 2016 Mar 4];448(1):189–97. Available from: http://www.sciencedirect.com/science/article/pii/S0378517313002482
24. Crucho CIC, Barros MT. Formulation of functionalized PLGA polymeric nanoparticles for targeted drug delivery. Polymer (Guildf) [Internet]. 2015 Jun [cited 2016 Feb 13];68:41–6. Available from: http://www.sciencedirect.com/science/article/pii/S0032386115004309
25. Jensen DK, Jensen LB, Koocheki S, Bengtson L, Cun D, Nielsen HM, et al. Design of an inhalable dry powder formulation of DOTAP-modified PLGA nanoparticles loaded with siRNA. J Control Release [Internet]. 2012 Jan 10 [cited 2016 Feb 13];157(1):141–8. Available from: http://www.sciencedirect.com/science/article/pii/S0168365911005797

26. John M, Jose B, Mendelsohn J, Baselga J. Epidermal growth factor receptor targeting in cancer. Semin Oncol [Internet]. 2006;33:369–85. Available from: http://linkinghub.elsevier.com/retrieve/pii/S0093775406001771

27. Lu Y, Li X, Liang K, Luwor R, Siddik ZH, Mills GB, et al. Epidermal growth factor receptor (EGFR) ubiquitination as a mechanism of acquired resistance escaping treatment by the anti-EGFR monoclonal antibody cetuximab. Cancer Res. 2007;67(17):8240–7.

28. Altintas I, Kok RJ, Schiffelers RM. Targeting epidermal growth factor receptor in tumors: from conventional monoclonal antibodies via heavy chain-only antibodies to nanobodies. Eur J Pharm Sci [Internet]. 2012 Mar 12 [cited 2016 Jan 12];45(4):399–407. Available from: http://www.sciencedirect.com/science/article/pii/S092809871100368X

29. Herbst RS, Shin DM. Monoclonal antibodies to target epidermal growth factor receptor-positive tumors a new paradigm for cancer therapy. Cancer. 2002;94(5):1593–611.

30. Maya S, Sarmento B, Lakshmanan V-K, Menon D, Seabra V, Jayakumar R. Chitosan cross-linked docetaxel loaded EGF receptor targeted nanoparticles for lung cancer cells. Int J Biol Macromol [Internet]. 2014 Aug [cited 2016 Feb 13];69:532–41. Available from: http://www.sciencedirect.com/science/article/pii/S0141813014003924

31. Kutty RV, Feng S-S. Cetuximab conjugated vitamin E TPGS micelles for targeted delivery of docetaxel for treatment of triple negative breast cancers. Biomaterials [Internet]. 2013 Dec [cited 2016 Feb 15];34(38):10160–71. Available from: http://www.sciencedirect.com/science/article/pii/S0142961213011265

32. Perri F, Muto P, Schiavone C, Ionna F, Aversa C, Maiolino P, et al. 583 Induction Chemotherapy with Docetaxel, Cisplatin and Capecitabine, Followed by Combined Cetuximab and Radiotherapy in Patients with Locally Advanced Inoperable Head and Neck Cancer. Preliminary Results of a Phase I/II Study. Eur J Cancer [Internet]. 2012 Nov [cited 2016 Feb 11];48:178–9. Available from: http://www.sciencedirect.com/science/article/pii/S0959804912723808

33. Govindan R. Cetuximab in advanced non-small cell lung cancer. Clin Cancer Res [Internet]. 2004;10(12 Pt 2):4241s – 4244s. Available from: http://www.ncbi.nlm.nih.gov/pubmed/15217966

34. El-Sayed IH, Huang X, El-Sayed MA. Surface plasmon resonance scattering and absorption of anti-EGFR antibody conjugated gold nanoparticles in cancer diagnostics: Applications in oral cancer. Nano Lett. 2005;5(5):829–34.

35. Dienstmann R, Martinez P, Felip E. Personalizing therapy with targeted agents in non-small cell lung cancer. Oncotarget [Internet]. 2011;2(3):165–77. Available from: http://www.pubmedcentral.nih.gov/articlerender.fcgi?artid=3260814&tool=pmcentrez&rendertype=abstract

36. Tabernero J. The Role of VEGF and EGFR Inhibition: Implications for Combining Anti–VEGF and Anti–EGFR Agents. Mol Cancer Res. 2007;5(3):203–20.

37. Thienelt CD, Bunn P a, Hanna N, Rosenberg A, Needle MN, Long ME, et al. Multicenter phase I/II study of cetuximab with paclitaxel and carboplatin in untreated patients with stage IV non-small-cell lung cancer. J Clin Oncol [Internet]. 2005;23(34):8786–93. Available from: http://www.ncbi.nlm.nih.gov/pubmed/16246975

38. Kurai J, Chikumi H, Hashimoto K, Yamaguchi K, Yamasaki A, Sako T, et al. Antibody-dependent cellular cytotoxicity mediated by cetuximab against lung cancer cell lines. Clin Cancer Res [Internet]. 2007;13(5):1552–61. Available from: http://www.ncbi.nlm.nih.gov/pubmed/17332301

39. Murakami H, Kobayashi M, Takeuchi H, Kawashima Y. Preparation of poly(dl-lactide-co-glycolide) nanoparticles by modified spontaneous emulsification solvent diffusion method. Int J Pharm [Internet]. 1999 Oct [cited 2016 Feb 13];187(2):143–52. Available from: http://www.sciencedirect.com/science/article/pii/S0378517399001878

40. Graves RA, Ledet GA, Glotser EY, Mitchner DM, Bostanian LA, Mandal TK. Formulation and evaluation of biodegradable nanoparticles for the oral delivery of fenretinide. Eur J Pharm Sci [Internet]. 2015 Aug 30 [cited 2016 Feb 13];76:1–9. Available from: http://www.sciencedirect.com/science/article/pii/S0928098715001797

41. Elzoghby AO, Samy WM, Elgindy NA. Albumin-based nanoparticles as potential controlled release drug delivery systems. J Control Release [Internet]. 2012 Jan [cited 2015 Oct 16];157(2):168–82. Available from:

http://www.sciencedirect.com/science/article/pii/S016836591100558X

42. Chaudhary H, Kohli K, Amin S, Rathee P, Kumar V. Optimization and formulation design of gels of Diclofenac and Curcumin for transdermal drug delivery by Box-Behnken statistical design. J Pharm Sci [Internet]. 2011 Feb [cited 2016 Mar 4];100(2):580–93. Available from: http://www.sciencedirect.com/science/article/pii/S0022354915322930
43. Singh B, Dahiya M, Saharan V, Ahuja N. Optimizing drug delivery systems using systematic "design of experiments." Part II: retrospect and prospects. Crit Rev Ther Drug Carrier Syst. 2005;22(3):215–94.
44. Chung Y-I, Kim JC, Kim YH, Tae G, Lee S-Y, Kim K, et al. The effect of surface functionalization of PLGA nanoparticles by heparin- or chitosan-conjugated Pluronic on tumor targeting. J Control Release [Internet]. 2010 May 10 [cited 2016 Feb 13];143(3):374–82. Available from: http://www.sciencedirect.com/science/article/pii/S0168365910000477
45. Kulhari H, Kulhari DP, Singh MK, Sistla R. Colloidal stability and physicochemical characterization of bombesin conjugated biodegradable nanoparticles. Colloids Surfaces A Physicochem Eng Asp [Internet]. 2014 Feb [cited 2016 Feb 13];443:459–66. Available from: http://www.sciencedirect.com/science/article/pii/S092777571300928X
46. Abdelwahed W, Degobert G, Stainmesse S, Fessi H. Freeze-drying of nanoparticles: Formulation, process and storage considerations. Advanced Drug Delivery Reviews. 2006. p. 1688–713.
47. Beck-Broichsitter M, Schmehl T, Gessler T, Seeger W, Kissel T. Development of a biodegradable nanoparticle platform for sildenafil: formulation optimization by factorial design analysis combined with application of charge-modified branched polyesters. J Control Release [Internet]. 2012 Feb 10 [cited 2016 Mar 4];157(3):469–77. Available from: http://www.sciencedirect.com/science/article/pii/S0168365911008431
48. Wang X-B, Zhou H-Y. Molecularly targeted gemcitabine-loaded nanoparticulate system towards the treatment of EGFR overexpressing lung cancer. Biomed Pharmacother = Biomédecine pharmacothérapie [Internet]. 2015 Mar [cited 2016 Feb 11];70:123–8. Available from: http://www.sciencedirect.com/science/article/pii/S0753332215000232

49. Morachis JM, Mahmoud E a, Almutairi A. Physical and chemical strategies for therapeutic delivery by using polymeric nanoparticles. Pharmacol Rev [Internet]. 2012;64(3):505–19. Available from: http://www.pubmedcentral.nih.gov/articlerender.fcgi?artid=3400833&tool=pmcentrez&rendertype=abstract

50. Fang C, Bhattarai N, Sun C, Zhang M. Functionalized nanoparticles with long-term stability in biological media. Small. 2009;5(14):1637–41.

51. Carlsson N, Borde A, Wölfel S, Kerman B, Larsson A. Quantification of protein concentration by the Bradford method in the presence of pharmaceutical polymers. Anal Biochem. 2011;411(1):116–21.

52. Hammond JB, Kruger NJ. The bradford method for protein quantitation. Methods Mol Biol. 1988;3:25–32.

53. Compton SJ, Jones CG. Mechanism of dye response and interference in the Bradford protein assay. Anal Biochem. 1985;151(2):369–74.

54. Jain A, Thakur K, Kush P, Jain UK. Docetaxel loaded chitosan nanoparticles: formulation, characterization and cytotoxicity studies. Int J Biol Macromol [Internet]. 2014 Aug [cited 2016 Feb 15];69:546–53. Available from: http://www.sciencedirect.com/science/article/pii/S0141813014004127

55. Du P, Li N, Wang H, Yang S, Song Y, Han X, et al. Development and validation of a rapid and sensitive UPLC-MS/MS method for determination of total docetaxel from a lipid microsphere formulation in human plasma. J Chromatogr B Analyt Technol Biomed Life Sci [Internet]. 2013 May 1 [cited 2016 Feb 21];926:101–7. Available from: http://www.sciencedirect.com/science/article/pii/S1570023213000913

56. Venishetty VK, Parikh N, Sistla R, Ahmed FJ, Diwan PV. Application of validated RP-HPLC method for simultaneous determination of docetaxel and ketoconazole in solid lipid nanoparticles. J Chromatogr Sci. 2011;49(2):136–41.

57. Fliszar K, Wiggins JM, Pignoli CM, Martin GP, Li Z. Analysis of organic volatile impurities in pharmaceutical excipients by static headspace capillary gas chromatography. In: Journal of Chromatography A. 2004. p. 83–91.

58. Fonte P, Reis S, Sarmento B. Facts and evidences on the lyophilization of polymeric nanoparticles for drug delivery. J Control Release [Internet]. 2016 Jan 21 [cited 2016 Feb 7];225:75–86. Available from:

http://www.sciencedirect.com/science/article/pii/S0168365916300311

59. Tang X, Pikal MJ. Design of Freeze-Drying Processes for Pharmaceuticals: Practical Advice. Pharmaceutical Research. 2004. p. 191–200.

60. Win KY, Feng S-S. Effects of particle size and surface coating on cellular uptake of polymeric nanoparticles for oral delivery of anticancer drugs. Biomaterials. 2005;26(15):2713–22.

61. Zou W, Liu C, Chen Z, Zhang N. Studies on bioadhesive PLGA nanoparticles: A promising gene delivery system for efficient gene therapy to lung cancer. Int J Pharm [Internet]. 2009 Mar 31 [cited 2016 Feb 13];370(1-2):187–95. Available from: http://www.sciencedirect.com/science/article/pii/S0378517308007825

62. Makadia HK, Siegel SJ. Poly Lactic-co-Glycolic Acid (PLGA) as biodegradable controlled drug delivery carrier. Polymers (Basel). 2011;3(3):1377–97.